Journal of Building Engineering 132 (2026) 117314

Contents lists available at ScienceDirect

Journal of Building Engineering

journal homepage: www.elsevier.com/locate/jobe

Textile reinforcement mortar: Natural fiber TRM system for integrated (structural and thermal) retrofitting

Arnas Majumder [a,*], Monica Valdes [a], Giovanna Concu [a], Andrea Frattolillo [a], Maria Francesca Sabbà [b], Marco Pepe [c], Flavio Stochino [a]

[a] Department of Civil Environmental Engineering and Architecture, University of Cagliari, via Marengo 2, Cagliari, CA, 09123, Italy
[b] Department of Architecture, Construction and Design, Polytechnic University of Bari, via E. Orabona 4, Bari, BA, 70125, Italy
[c] Department of Civil Engineering, University of Salerno, via Giovanni Paolo II n.132, Fisciano, SA, 84084, Italy

A R T I C L E I N F O

Keywords:
Integrated retrofitting
Integrated upgrading
Structural retrofitting
Structural upgrading
Thermal retrofitting
Thermal upgrading
Flax fiber
Natural fiber

A B S T R A C T

The retrofit of existing masonry buildings requires solutions capable of simultaneously improving structural safety and energy efficiency while reducing environmental impacts. Although Textile Reinforced Mortar (TRM) systems are widely used for structural strengthening, integrated thermo-structural solutions based on natural and recycled materials remain largely unexplored. This study investigates an innovative Natural Fiber Textile Reinforced Mortar (NFTRM) system combining flax fiber textiles, sheep-wool insulating mortars, jute-fiber diatons, and recycled fine aggregates for the integrated upgrading of masonry walls. An experimental campaign was conducted on eighteen masonry wall specimens representing six retrofit configurations. To enhance sustainability, 30% of the natural sand was replaced with recycled fine aggregates (recycled sand) derived from construction and demolition waste. Thermal performance was assessed using a climate chamber, while structural behavior was evaluated through diagonal compression tests. The results demonstrate significant improvements in both thermal and mechanical performance compared with the unreinforced reference walls. The combined textile-and-insulation system (TRMTL) achieved the highest thermal enhancement, increasing thermal resistance by 73.7%, while TRMTLD and TRMD improved thermal resistance by 54.7% and 48.1%, respectively. Structurally, the retrofitted walls exhibited increases in load-bearing capacity ranging from 17.5% to 59.3% compared with unreinforced masonry, with the best performance achieved by diaton-enhanced configurations. The proposed NFTRM systems successfully combine structural strengthening, thermal insulation, and circular-economy principles by bio-based and recycled materials. These findings demonstrate the potential of sustainable NFTRM solutions as an effective strategy for the integrated seismic and energy retrofit of existing masonry buildings.

1. Introduction

According to the UN Environment Program (UNEP) and the Global Alliance for Buildings and Construction (GlobalABC) report (2024/2025) [1], the Construction and Building (C&B) sector consumes about 32% of the total global energy use. Whereas C&B is also responsible for contributing to 34% of global CO_2 emissions [1].

* Corresponding author.
E-mail address: arnas.majumder@unica.it (A. Majumder).

https://doi.org/10.1016/j.jobe.2026.117314
Received 9 July 2026; Received in revised form 3 September 2026; Accepted 9 September 2026
Available online 19 September 2026

Masonry structures represent a substantial portion of the global building stock [2]. While a significant number (about 70%) of these buildings are Unreinforced Masonry Buildings (UMB) [3], and they can be found in seismically active, historic cities [4]. In most cases, these buildings are found to have poor structural performance under seismic activity, and the majority of them are not energy efficient; therefore, they require urgent attention [5]. The majority of these buildings have been designed for construction with only vertical loads considered [6]. Existing retrofitting techniques have mostly focused on structural and thermal retrofitting separately [7]. The latter approach results in a higher costs and reduced effectiveness. Actually, retrofitting/upgrading is pivotal to achieving energy-efficient buildings [1]. These buildings urgently need seismic [8] and thermal [8–10] upgrades required by EU directives [8, 11], which also promote fire safety and thermal-structural retrofitting.

Various Fiber Reinforced Polymer (FRP) techniques [11–17] have been widely used for masonry structural retrofitting/upgrading [18]. Meanwhile, Textile Reinforced Mortar (TRM) has recently emerged as a widely adopted strategy for masonry retrofitting [19–23]. Textile Reinforced Mortar (TRM) is considered one of the most effective methods for strengthening masonry buildings and structures due to its multiple advantages (TRM employs an inorganic matrix, offers improved ductility, fire resistance, breathability, and easier application, while reducing stress concentration and maintaining performance at high temperatures) over FRPs [6]. Moreover, TRM is highly compatible with historic materials [24]. At the same time, the use of natural and recycled materials in construction is increasing, driven by growing awareness of environmental issues and supporting the circular economy. Natural fibers such as flax [25], jute [26], coconut [27], date-palm [28], bamboo [29], rice husk [30], and sheep wool [31] are considered good sustainable alternatives due to their lower production energy requirements, renewability, and favorable mechanical and thermal qualities. Several notable studies investigated Natural Fiber TRM (NFTRM) for structural strengthening-using flax [32], hemp [33], jute [34]-as well as bio-based materials [35–39] for thermal insulation separately. there is little research on retrofitting solutions that combine both aspects in a single layer. Integrated retrofitting is an innovative approach to upgrading masonry structures both structurally and thermally simultaneously. Based on the literature review, it has been observed that in this type of retrofitting strategy, researchers have used particularly man-made/fibers like glass, steel, and basalt fiber nets used as the structural retrofitting material, and EPS, ETICS, RTIM were used as the thermal retrofitting material [40–46]. The recent advancements in computational techniques have indicated the capability of machine learning and genetic programming to predict the mechanical properties of sustainable cement-based materials [47–50]. Such techniques will be beneficial not only for the optimization of materials but also for developing predictive techniques for sustainable construction materials.

While the use of natural fibers for integrated retrofitting is very rare, Stochino et al. (2025) [51] have reported being the first to have used the NFTRM package, consisting of jute fiber net, jute fiber diatons, and jute fiber composite mortar for structural (525% increase in load-bearing capacity) as well as thermal (36.05% reduction in thermal transmittance) retrofitting. No dedicated standards are currently available for designing, testing, and/or qualifying the natural fiber TRM system. Therefore, most researchers follow the standard and guidelines of RILEM TC 250-CSM (2016) [52], ACI 549.4R-13 (2013) [53], developed in the United States (US), and CNR-DT (2018) [54], developed by the Italian National Research Council (CNR). Furthermore, to the best of the authors' knowledge,

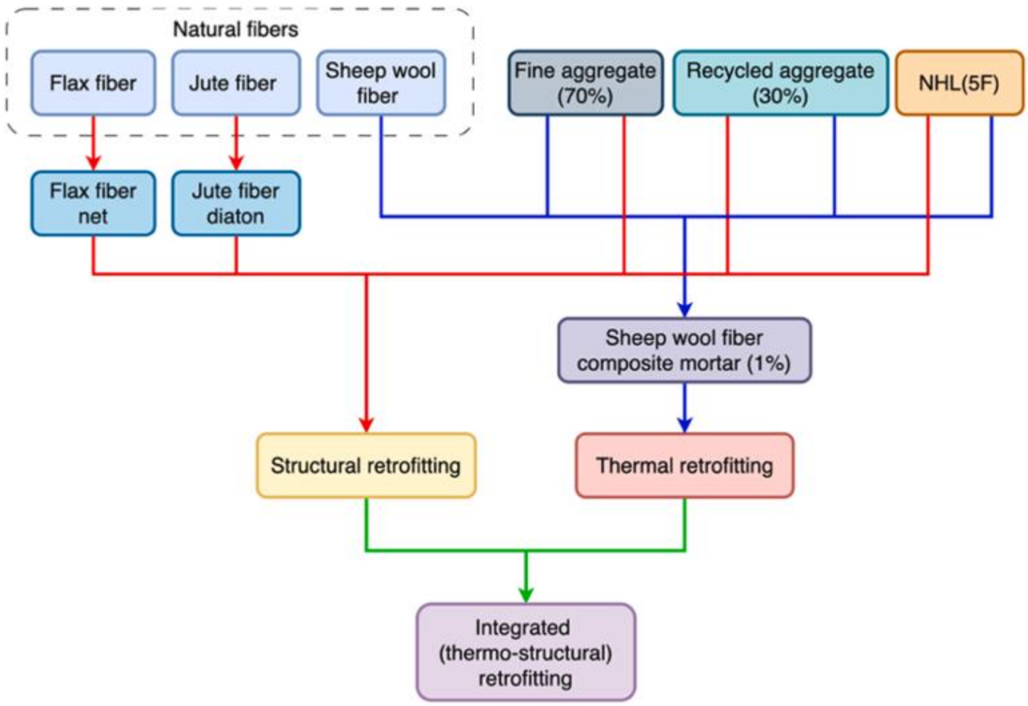

Fig. 1. Masonry walls retrofitting scheme.

no studies have investigated the combined use of flax fiber net, insulating mortars containing sheep wool fibers, and jute fiber diatons for retrofitting or upgrading. Therefore, this is the first time their joint thermal and structural, i.e., integrated behavior has been explored.

The main contributions of this study are: (1) The use of natural fibers (flax, sheep wool, and jute) and 30% recycled aggregate (derived from demolition sites) for masonry wall retrofitting/upgrading purposes, and (2) Thermo-structural performance evaluation. For retrofitting/upgrading, flax fiber net, composite mortars manufactured from sheep wool fiber and either natural or recycled aggregates, jute fiber diaton, have been used. Different masonry wall retrofitting/upgrading configurations have been used: (1) Thermal layers (TL) system; (2) TRM system; (3) TRM-TL combined system, and (4) Diaton (D) enhanced TRM system (TRMD and TRMTLD).

All masonry walls are subjected to structural and thermal tests to evaluate the thermo-structural (integrated) performance. Masonry wall specimens were subjected to diagonal compression tests in accordance with ASTM E519/E519M – 22 [55] to evaluate and compare their in-plane shear behavior and the effectiveness of the different retrofit configurations under this loading condition. Whereas, thermal conductance tests and thermal properties were evaluated using UNI EN ISO 9869-1:2014 [56], UNI EN ISO 8990:1996 [57], UNI EN ISO 10456:2008 [58].

This research was developed as part of the PRIN PNRR 2022 "IntegraTRM" project that supports the United Nations Sustainable Development Goals (UNSDGs) [59], as it promotes the use of sustainable, bio-based, and recyclable natural raw materials in a complete and cohesive way as part of the integrated retrofitting strategy. The findings of this experimental campaign are important for developing new retrofitting and upgrading strategies for masonry buildings and structures aimed at improving structural safety, energy efficiency, sustainability, and other key aspects in both new construction and heritage properties, while employing environmentally responsible construction methods.

2. Materials and methods

During the "IntegraTRM" project's experimental campaign, a total of eighteen "60 cm × 60 cm" masonry walls have been constructed. For retrofitting/upgrading masonry walls, see Fig. 1, several sustainable materials and combinations have been employed, including flax fiber net, composite mortars manufactured from sheep wool fiber combined with either natural or recycled aggregates, and jute fiber diatons. Several retrofitting/upgrading configurations have been explored, such as the Thermal Layers (TL) system, the Textile Reinforced Mortar (TRM) system, the combined TRMTL system, and the Diaton-enhanced TRM system, including TRMD and TRMTLD configurations.

2.1. Raw materials and the selection of optimum mixtures

Fig. 2 shows the main materials used during Phase I: material characterization, and Phase II: retrofitting/upgrading the masonry

Fig. 2. (a) Clay bricks, (b) flax net, (c) natural sand, (d) NHL(5F) natural hydraulic lime, (e) recycled sand, (f) chopped sheep wool, and (g) jute fiber diaton.

wall specimens.

Clay bricks of dimensions 25 cm × 12 cm x 5 cm (Fig. 2a) have been used for the construction of all masonry wall specimens, while flax fiber net (Fig. 2b) has been used for strengthening wall samples. The mortars are composed of Natural Sand (NS) (Fig. 2c), hydraulic lime-NHL(5F) (Fig. 2d), and Recycled Sand (RS) used as a sustainable alternative aggregate (Fig. 2e). Chopped sheep wool (Fig. 2f) has been incorporated into the composite mortar to enhance the thermal performance of the wall systems. Additionally, jute fiber diatons (Fig. 2g) have been used as transverse connectors to improve through-thickness mechanical behavior and overall structural integrity.

Flax-fiber net: The NFL-NET 300 BA flax-fiber net [60] acts as the principal distributed tensile reinforcement within the proposed NFTRM system. The textile is characterized by a 10 × 10 mm mesh, nominal yarn area of 0.931 mm^2, mass per unit area of 310 g/m^2, tensile strength of 216 MPa, tensile elastic modulus of 5306 MPa, elongation at failure of 4.3%, and breaking load of 20.5 kN/m per direction. These mechanical characteristics enable the flax textile to provide tensile reinforcement after cracking, redistribute tensile stresses, and contribute to crack control within the reinforced mortar layer. Thus, its contribution to the proposed system is predominantly structural, providing distributed in-plane reinforcement to the masonry surface.

Sardinian sheep-wool fibers: The Sardinian sheep-wool fibers are incorporated primarily to improve the thermal characteristics of the composite mortar. As reported in Ref. [61], they have an average fiber diameter of approximately 41.0 μm and an average fiber length of approximately 125.2 mm. In addition, locally produced Sardinian sheep-wool insulation has demonstrated favorable thermal properties for building applications. The technical characterization of the Brebey Tecnolana sheep-wool insulation product reports a thermal conductivity (λ) of about 0.040 W/(m·K) [62], determined according to UNI EN ISO 12667:2002 [63].

Jute-fiber diatons: Detailed information about the diatons specification is reported in authors previous experimental campaign [64]. The jute-fiber diatons serve primarily as transverse mechanical connectors between the reinforcement layers applied to the opposite surfaces of the masonry wall. As in Ref. [64], the mechanical characteristics of average tensile strength of 15.54 MPa, strain energy of 14.18 kN mm, and axial strain of approximately 0.03 have been reported. Individual diaton specimens exhibited tensile failure loads ranging from approximately 2.09 to 3.92 kN. The jute diatons are used to create a connection in thickness, ensuring the integration of the faces that have been reinforced. In this sense, their role becomes complementary to that of the flax textile.

Recycled sand: The recycled sand (RS) used in this study was obtained from construction and demolition waste in Cagliari. Previous characterization of the same recycled aggregate source [65] reported a maximum particle size of 5.0 mm, water absorption of 12.9%, and dry density of 2240 kg/m^3. The relatively high water absorption of the recycled aggregate is associated with the presence of adhered residual mortar and a more porous and heterogeneous structure, which can influence its interaction with the surrounding mortar matrix and the resulting mechanical performance.

The choice of 1% (in volume) sheep wool fiber is based on two factors: (1) the author's experience from previous studies [51,64,66], and (2) the limitations provided by the EN 13501-1, which highlights that the presence of fiber must be lower than or equal to 1% in an incombustible composite mixture [67].

Two types of specimens have been prepared (EN 1015-2 [68] and EN 1015-3 [69]): "160 mm × 40 mm x 40 mm" (three for each mix), as in Fig. 3(a), and "160 mm × 140 mm x 40 mm" (two for each mix), as in Fig. 3(b), were prepared to evaluate the mechanical (flexural and compression tests) and thermal (thermal conductivity tests) properties, when NS was replaced with 30%, 50%, 70%, and 100% of RS.

A three-point bending flexural test was performed according to EN 1015-11 [70] using a displacement-controlled Metrocom-1 machine with a 5 kN load capacity and 0.02 kN sensitivity. A class 1 load cell (1-ton capacity, 2 mV/V sensitivity) and an LVDT sensor (50 mm range, 2 mV/V sensitivity, <0.10% linearity error) were used to measure force and displacement. Compression tests [70] were carried out using a load-controlled Metrocom-2 machine with a 40 kN capacity. Fig. 4 (a) represents the flexural strength test of a sample with 70% NS and 30% RS after collapse, while Fig. 4 (b) shows the collapsed sample after the compressive strength test.

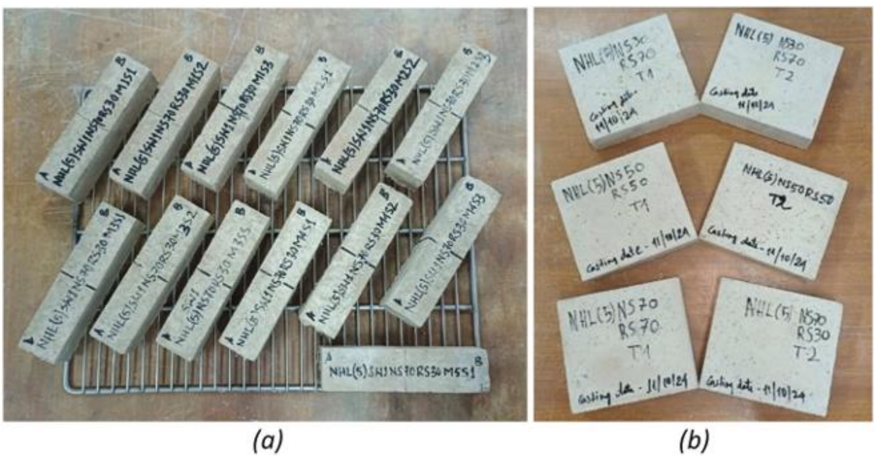

Fig. 3. Specimens used to evaluate: (a) mechanical, and (b) thermal properties.

The findings from the mechanical tests are shown in Fig. 5. Specimens with 30% RS replacement were found to be the best performers, exhibiting the highest flexural strength (Fig. 5a) and second-highest compression strength (Fig. 5b).

For Thermal conductivity (TC) tests, the samples were oven-dried to constant mass in order to eliminate the influence of moisture on the measurements (Fig. 6a). The TC measurements were performed using a heat flow meter apparatus, which has a controlled testing chamber equipped with a movable hot plate and a fixed cold plate (Fig. 6b). During testing, the sample was placed between the two plates within the active measurement zone (10 cm × 10 cm), ensuring one-dimensional heat transfer through the specimen thickness. A wool heat guard layer was placed around the sample to minimize lateral heat losses, as shown in Fig. 6c. A steady-state temperature gradient was imposed between the hot and cold plates, and the resulting heat flux was measured to determine the thermal conductivity of the specimens. Fig. 7 presents the thermal conductivity values of the tests conducted on the specimens with 100% NS, and those when NS was replaced with 30%, 50%, and 70% of RS. For TC tests, samples with 100 RS have not been prepared, as there was no intention to retrofit/upgrade the masonry walls with 100% recycled aggregates.

The goal of the aforementioned tests was to identify the mixture providing the optimum balance between mechanical and thermal performance.

The experimental findings demonstrated that the samples with 30% RS have demonstrated the most favorable thermo-mechanical balance among the replacement levels investigated, exhibiting the highest flexural strength, the second-highest compressive strength, and suitable thermal performance. At moderate replacement levels, recycled sand can be incorporated while maintaining adequate mechanical performance; however, increasing the RS content progressively introduces a greater proportion of recycled particles into the mortar.

Recycled particles generally contain a certain amount of adhered old mortar and possess higher porosity and a more heterogeneous surface structure than natural aggregates. These characteristics may lead to a less compact and more heterogeneous matrix and weaker interfacial transition zones (ITZs) between the recycled particles and the surrounding binder.

In addition, the presence of residues of mortar, along with micro-cracks, which were inherent with the recycled aggregates, would help the crack formation and development, leading to the decrease in the compressive and flexural properties when the percentage of RS was relatively high [71]. Regarding the heat transfer, the increased porosity due to the presence of the recycled aggregate could affect the thermal conductivity of the mortar.

Therefore, 30% RS should not be considered a universal optimum replacement ratio, but rather it should be considered as the optimum thermo-mechanical balance identified for the materials, mixture proportions, and replacement levels, and objective integrated-performance criterion adopted iin the present study. Accordingly, the mixture containing 30% RS as a replacement for NS was selected for the subsequent masonry wall retrofitting/upgrading campaign.

2.2. Masonry retrofitting/upgrading

Table 1 presents the short form, nomenclature, and summarizes the masonry wall configurations investigated, considering both geometric size and strengthening/insulation solutions. Two wall panel sizes were used, identified as 60 (60 cm × 60 cm), with thicknesses ranging from 12 cm to 18 cm depending on the configuration. The reference walls (NR) consist of unreinforced masonry with a thickness of 12 cm. Retrofitted and/or insulated configurations have a total thickness of 18 cm and include: (a) walls with a Thermal Layer (TL) applied on both sides using sheep wool insulation embedded in composite mortar; (b) walls strengthened with Textile Reinforced Mortar (TRM), composed of mortar layers and a reinforcing net; (c) combined systems (TRM TL) integrating both textile reinforcement and the sheep wool-based thermal layer; and (d) further enhanced systems incorporating Diatons (D), which are transverse connectors improving through-thickness behavior, leading to TRMD and TRMTLD configurations. Fig. 8 illustrated sections (a–f) show the progression from plain masonry (NR), to insulated (TL), reinforced (TRM), reinforced–insulated (TRM TL), reinforced with diatons (TRM D), and reinforced–insulated with diatons (TRM TL D), clearly indicating the arrangement of masonry units, mortar, textile or flax nets, composite mortar layers, thermal insulation, and diatons.

Fig. 9 documents the materials preparation phase and the construction process of the masonry wall specimens. Mortar used for the

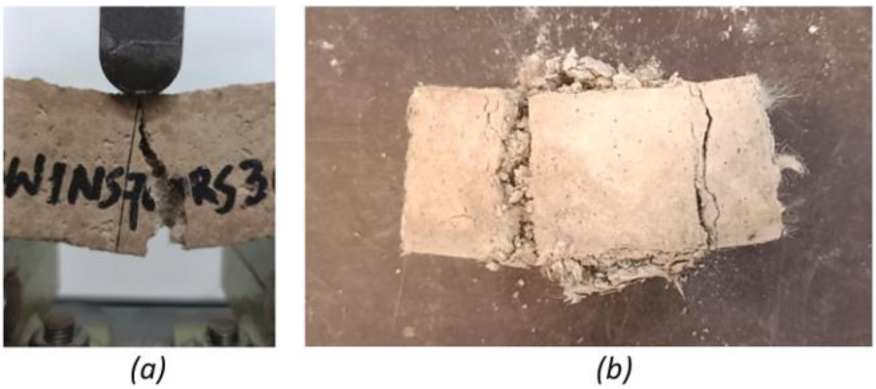

Fig. 4. Specimens after failure: (a) flexural strength test, and (b) Compressive strength test.

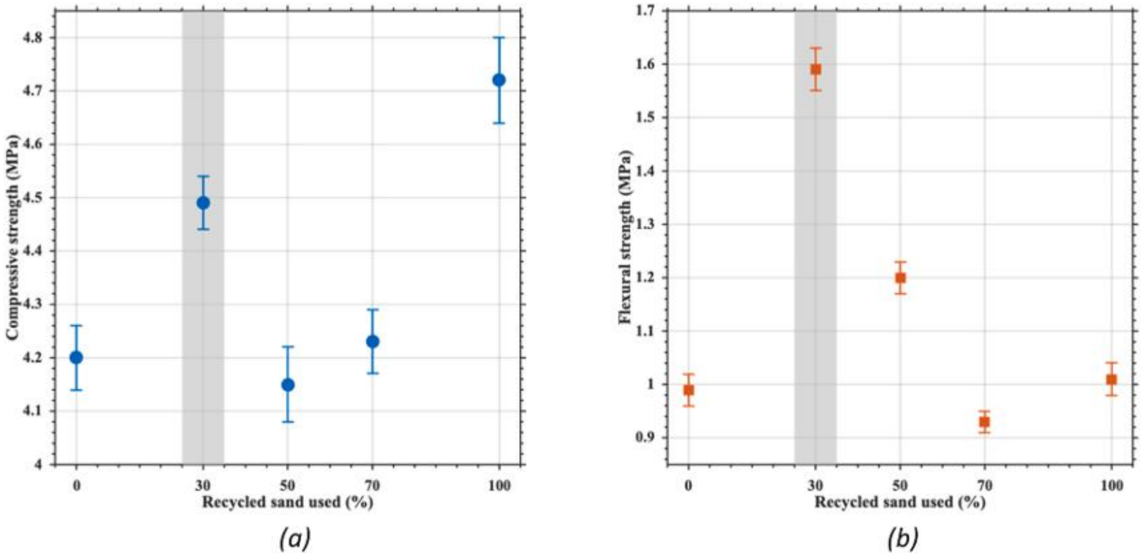

Fig. 5. (a) Compressive Strength and (b) Flexural Strength with variation of recycled sand percentage.

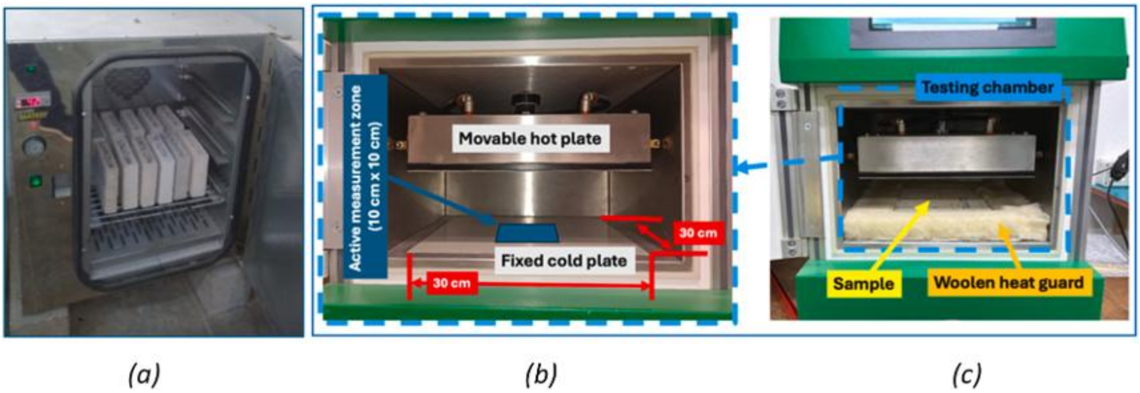

Fig. 6. Specimens (160 mm × 140 mm x 40 mm) for TC test, (a) oven drying, (b) Heat flow meter chamber, and (c) sample placed inside the chamber.

construction of non-reinforced masonry walls has been prepared using NHL(5), 70% NS, and 30% RS. The images illustrate the masonry assembly formwork (Fig. 9a), and on-site setup adopted to ensure consistent geometry (Fig. 9b), and construction quality across all wall configurations (Fig. 9c).

Sheep wool fibers used for the composite mortar preparation (70% NS and 30% RS) were soaked in water for approximately 3 to 4 h to achieve full saturation (Fig. 10 (a)), and then the excess trapped water was manually squeezed out (Fig. 10 (b)). This procedure was carried out to prevent the formation of fiber balls [64] and to ensure uniform fiber dispersion within the mixture. Fig. 10(c) illustrates the preparation of the composite mortar, in which sheep wool fibers were mixed to obtain an insulating mortar ideal to act as thermal layers.

Fig. 11 shows the flax textile nets (with mesh configuration dimension 1 cm × 1 cm (Fig. 11a) used for masonry retrofitting/upgrading, cut into a size of 60 cm × 60 cm (Fig. 11b), corresponding to the dimensions of the retrofitted/upgraded wall panels. Fig. 12 shows the thickness measurements of the retrofitting layer and masonry wall.

Fig. 12 (a) illustrates the wooden framework used to ensure a uniform plaster thickness, confirming the geometric consistency. Fig. 12 (b) shows the overall wall thicknesses after retrofitting. Notably, all walls exhibit a plaster thickness of 3 cm on both sides.

Fig. 13 depicts the masonry wall retrofitting/upgrading steps, on a specimen without diatons: it starts with the application of the first layer (1.5 cm) of mortar (70% NS and 30% RS)* (Fig. 13a), then flax nets have been placed on both sides (Fig. 13b), and finally, another layer (1.5 cm) of mortar (70% NS and 30% RS)* has been added (Fig. 13c).

The retrofitting/upgrading system with diaton starts with drilling a hole at the center (see Fig. 14a&b) of the masonry wall for the insertion of the diaton (see Fig. 14c). After the placement of diaton through the hole, a fast-drying liquid mortar was injected around the diaton to completely fill the gap (see Fig. 14d). Thereafter, a first layer (1.5 cm thick) of mortar (70% NS and 30% RS)* was applied

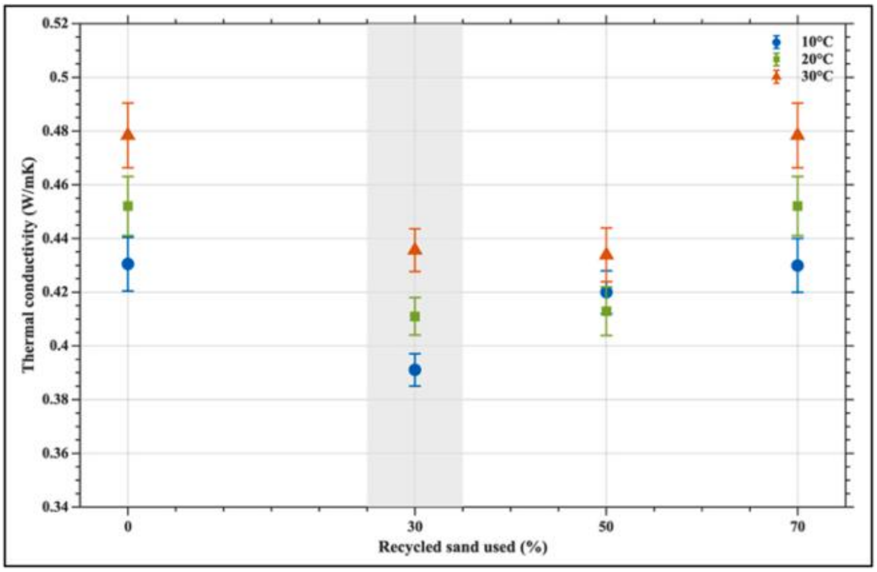

Fig. 7. Thermal conductivity test results.

Table 1
Masonry walls' configurations.

Shortforms	Nomenclatures	Thickness
	60 cm × 60 cm	12 cm for NR, and 18 cm for TL, TRM, TRMTL, TRMD, and TRMTLD
NR	No Reinforcement	12 cm
TL	Thermal Layer	18 cm
TRM	Textile Reinforced Mortar	18 cm
TRMTL	Textile Reinforced Mortar + Thermal Layer	18 cm
TRMD	Textile Reinforced Mortar + Diatons	18 cm
TRMTLD	Textile Reinforced Mortar + Thermal Layer + Diatons	18 cm

(see Fig. 14e) to fix the flax nets on both sides (see Fig. 14f). Thereafter, the diaton was opened to anchor nets (see Fig. 14g) on both sides. Finally, a second layer (1.5 cm thick) of mortar (70% NS and 30% RS)* was applied (see Fig. 14h).

* Please note: wall specimens with TL layers have 70% NS and 30% RS, plus 1% of sheep wool fiber.

2.3. *Thermo-structural tests*

Notably, the wall specimens were tested in the climate chamber to assess their insulating properties and later subjected to diagonal tension (shear) tests to evaluate their structural behavior.

2.3.1. *Masonry wall thermal characterization*

The thermal performance of the masonry walls was evaluated using the Biemme TH Climate Chamber (CC), as shown in Fig. 15.

The CC consists of three sections: two movable chambers and a central fixed wall, and it was built in compliance with the European standard EN 1934:2000 [72]. During each test, three masonry wall samples with dimensions of 60 cm × 60 cm × 12 cm (non--reinforced sample) and 60 cm × 60 cm x 18 cm (reinforced samples) respectively, were placed within the expandable polystyrene (EPS) frame which acts as a thermal guard to block and limit lateral heat losses (Fig. 16).

Fig. 17 shows a closer view of both the front (the indoor condition) and the back view (the outer condition) of a masonry specimen equipped with two heat fluxes and two temperature sensors (one pair on each side).

All experimental tests have been executed according to international standards to ensure consistency and reliability of the results. More specifically, they were performed according to the UNI EN ISO 9869-1:2014 [56] standard, which provides guidelines for in situ determination of thermal resistance and transmittance using heat flow meters, along with the criteria to ensure stability of the thermal regime and methods for data averaging. Tests of steady-state thermal transmission were carried out according to the UNI EN ISO 8990:1996 [57] standard, using a climatic chamber. Moreover, the determination of thermal properties was performed according to the UNI EN ISO 10456:2008 [58] standard, which specifies tabulated design values and standard methods for evaluating hygrothermal behavior. The climate chamber was built to provide two environmental conditions (see Fig. 18): indoor and OUTdoor, the warmer and cooler sides, respectively. Table 2 presents the limits/ranges of the settable test conditions of the climate chambers.

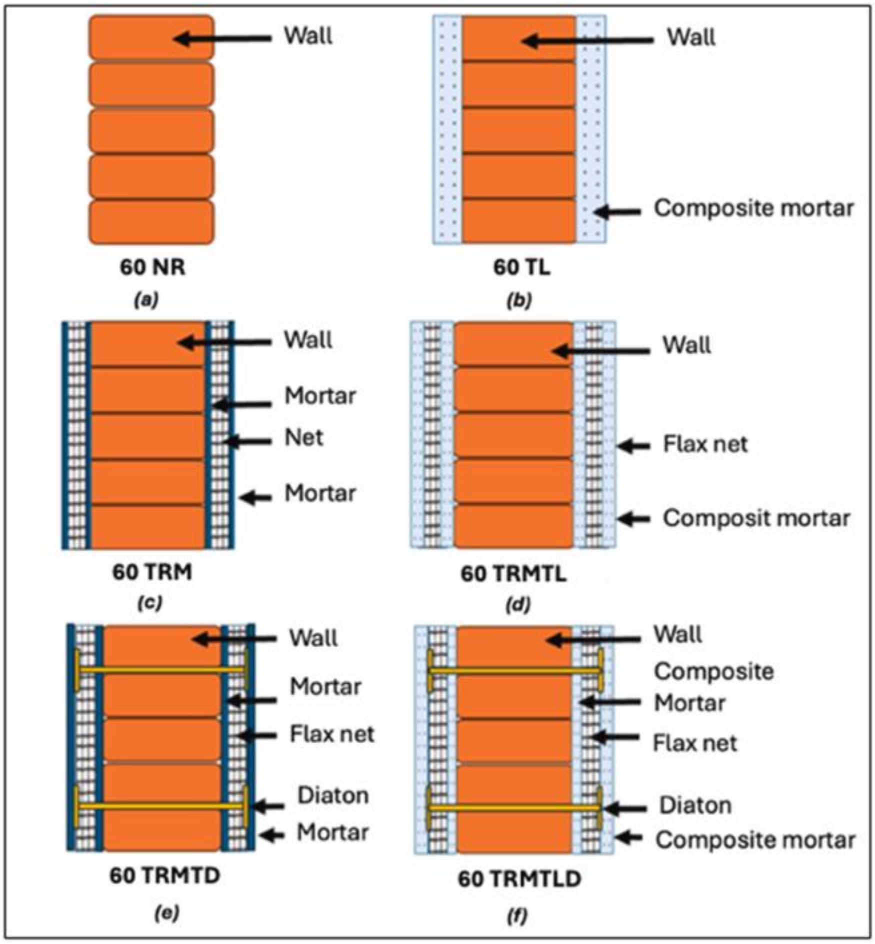

Fig. 8. Masonry walls' specifications: (a) NR, (b) TL, (c) TRM, (d) TRMTL, (e) TRMD, and (f) TRMTLD.

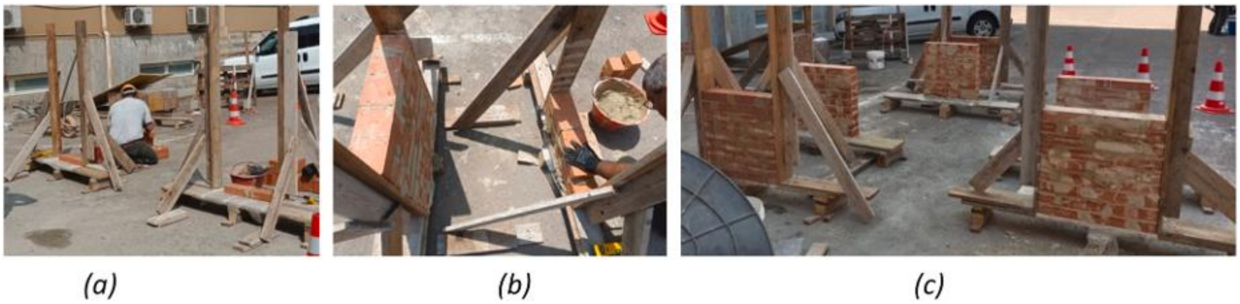

Fig. 9. (a) masonry assembly formwork, (b) Construction, and (c) un-strengthened masonry walls.

The thermodynamic characteristics of the tested samples were acquired using LSI heat flux meters (model DPE 240), whose performance characteristics are highlighted in Table 3, and using LSI surface temperature sensors, model DLE 124A (Pt100 1/3 DIN B Class AA), with an accuracy of 0.1°C.

The sensors were connected to a dedicated LSI E-LOG data acquisition system, equipped with 8 analogue inputs and 4 digital inputs (for pulse and frequency measurements). The internal 8 MB memory can store data for several weeks, depending on the number of connected sensors and the selected acquisition frequency.

Notably, the main aim of the current experiment is to make a consistent comparison of the thermal performance of the various wall samples under identical controlled boundary conditions. All wall samples with different retrofitting/upgrading schemes were tested under the same pre-selected conditions with an indoor temperature of 20°C, an outdoor temperature of 10°C, and a relative humidity

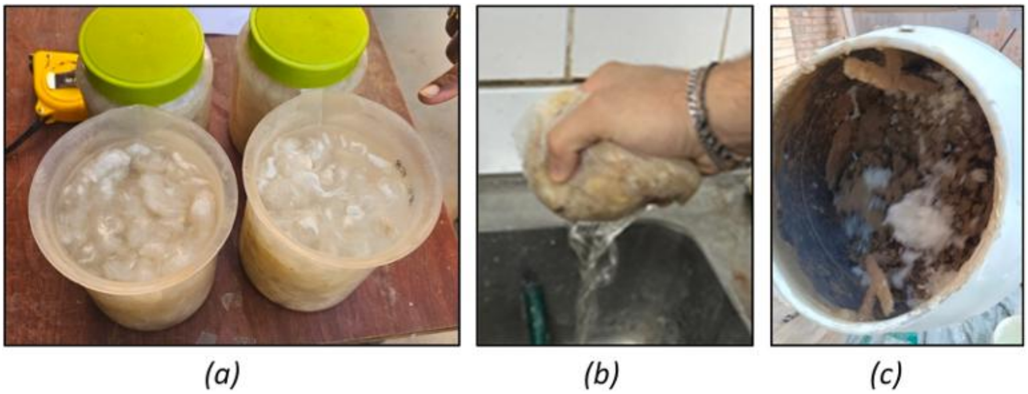

Fig. 10. (a) Sheep wool fiber, (b) squeezing out water from sheep wool, and (c) mortar mixture preparation with sheep wool.

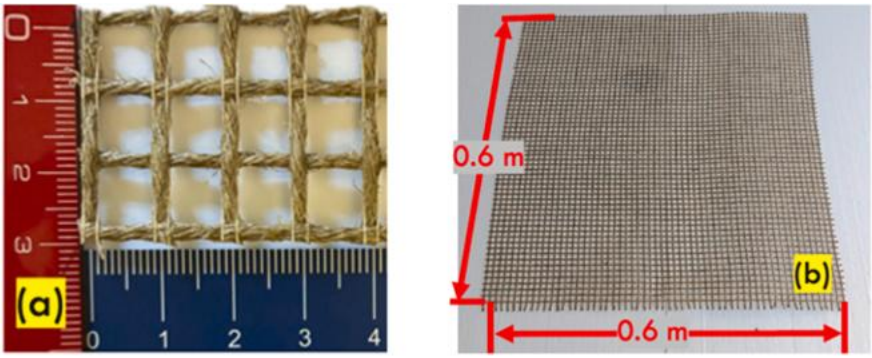

Fig. 11. (a) Flax net with a mesh configuration dimension of 1 cm × 1 cm, and (b) 60 cm × 60 cm flax net used for masonry retrofitting/upgrading.

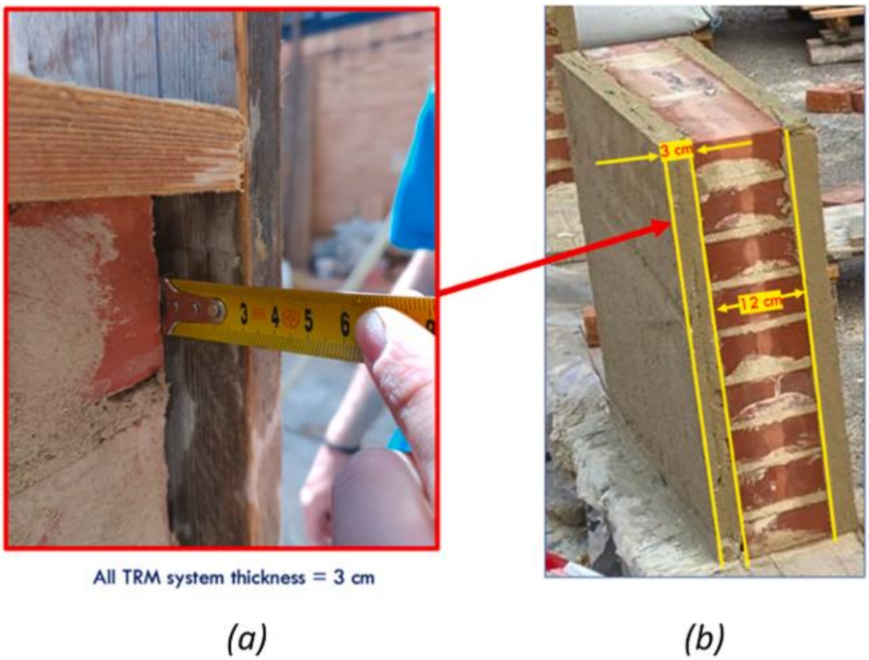

Fig. 12. (a) Thickness of the retrofitting layer, and (b) thickness of the masonry wall.

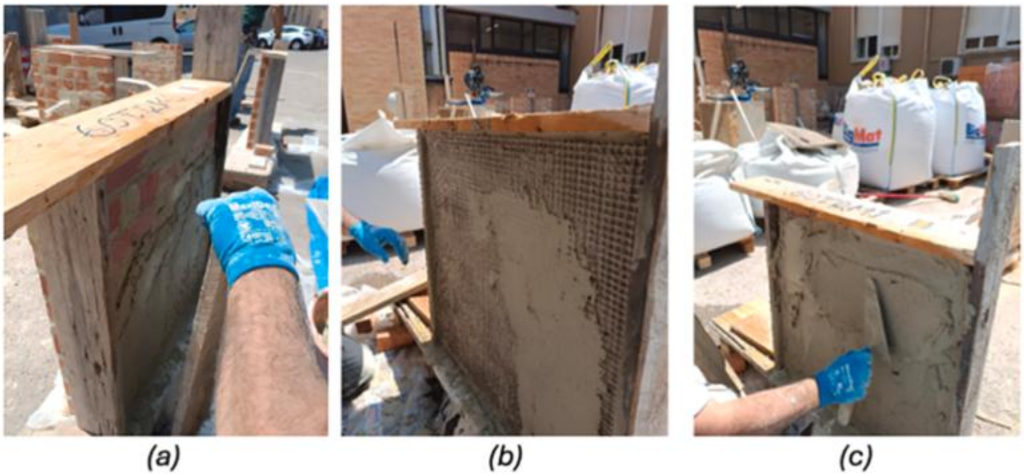

Fig. 13. Retrofitting without diaton, application of (a) mortar layer, (b) flax net, and (c) final mortar layer.

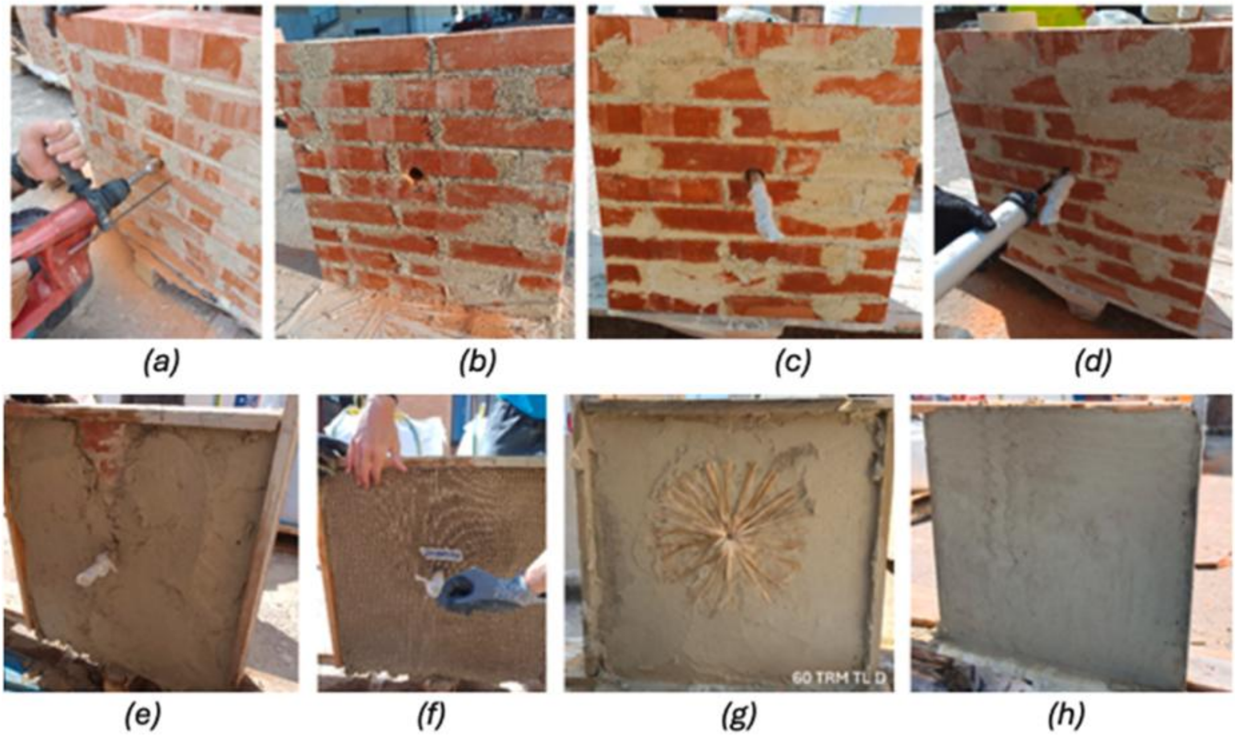

Fig. 14. Retrofitting with diaton: (a) Drilling a hole, (b) hole at the center, (c) placement of diaton, (d) injection of liquid mortar at gaps, (e) application of first layer of mortar, (f) application of net, (g) opening of diaton, and (h) application of final layer of mortar.

of 50%. The application of constant and repeatable boundary conditions was deliberately employed so as to reduce the effect of environmental changes on the test results.

2.3.2. Masonry wall structural characterization

Figs. 19 and 20 illustrate the experimental setup adopted for the structural characterization of the masonry wall specimens. Diagonal compression tests were performed in accordance with ASTM E519/E519M − 22 [55] to evaluate the shear behavior of the masonry assemblies.

The test setup consisted of a rigid steel loading frame in which the wall specimens were positioned diagonally and subjected to compressive loading along one diagonal, following the standard procedure. The load was applied using a double-acting Enerpac CLRG-504 hydraulic actuator with a maximum capacity of 500 kN (50 t) and a maximum operating pressure of 700 bar. Load transfer was

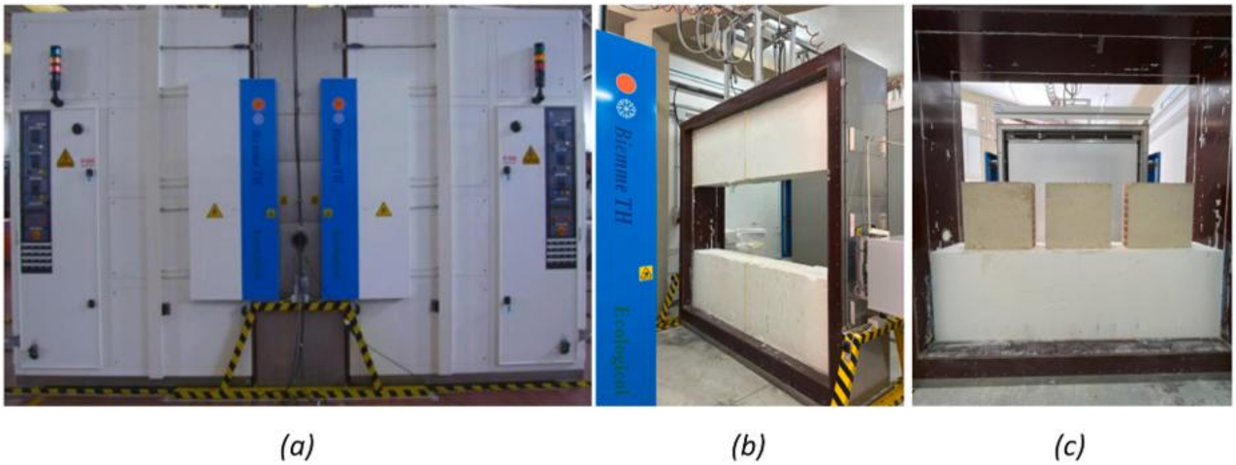

Fig. 15. (a) Climate chamber, (b) central chamber without wall specimens, and (c) central chamber with three wall specimens.

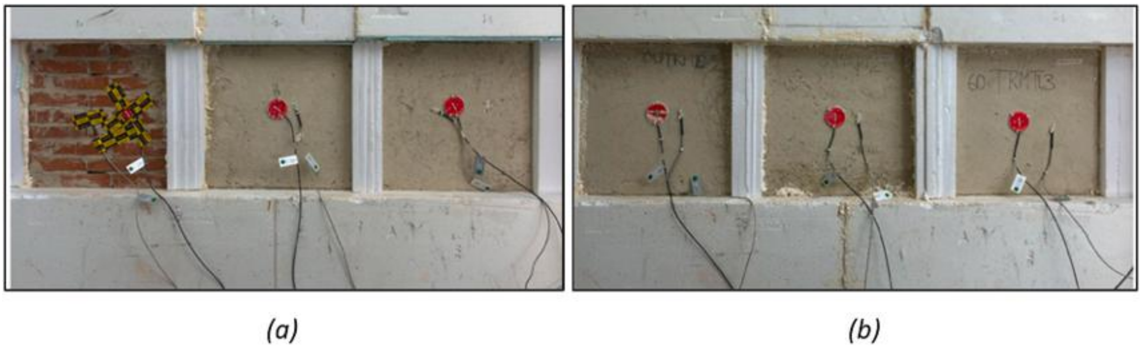

Fig. 16. Thermal conductivity test setup, wall specimens: (a) 60NR, 60TRMTLD, and 60 TL, and (b) 60TRMD, 60TRM, and 60TRMTL.

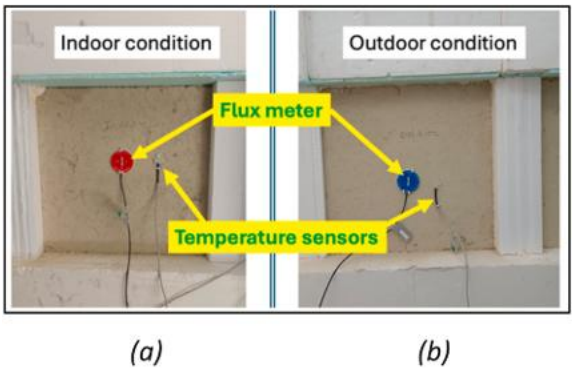

Fig. 17. Wall sample flux and temperature measurements on both sides: (a) front and (b) back.

achieved through two steel loading shoes placed at the top and bottom corners of the specimen, ensuring a uniform distribution of the applied force.

The applied force was measured using a TC4 strain-gauge load cells, suitable for both tension and compression, with a maximum capacity of 500 kN (50 tons), ISO 376 Class 1 accuracy, a nominal sensitivity of 2 mV/V, and IP67-rated stainless-steel construction. Diagonal deformations were recorded using two LDT strain-gauge displacement transducers with a 50 mm measurement range and a sensitivity of 2 mV/V. The sensors provided a resolution better than 1 μm, with linearity and hysteresis errors within ±0.10% of full scale. As shown in Fig. 19, one transducer was installed along the compressed diagonal and the other along the tension diagonal of the masonry panel. The recorded diagonal shortening and elongation were used to evaluate the shear deformation response of the

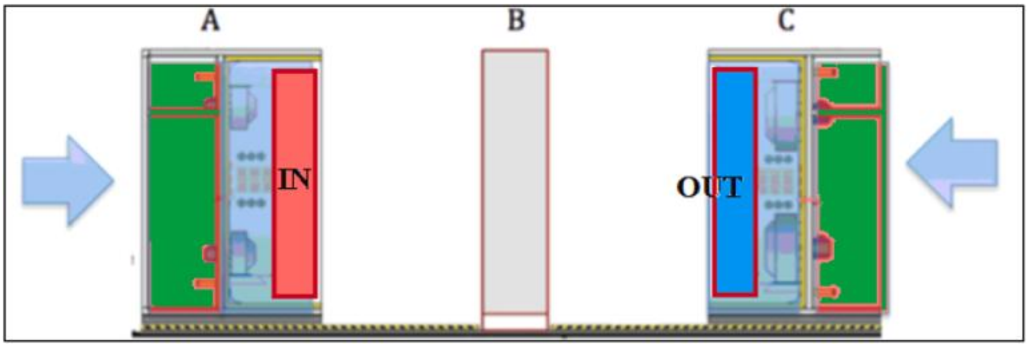

Fig. 18. Climate chamber configuration.

Table 2
Various ranges of the settable test conditions of the climate chambers.

Parameters measured by transducers and controlled by PLC		
	"INdoor" chamber	"OUTdoor" chamber
Part (Fig. 18)	A	C
Dry-bulb temperature:	from +15°C to +40°C	from −10°C to +80°C
Maximum temperature gradient (increase and decrease):	0.15 °C/min	
Relative humidity:	from 30% to 98% with dew point limitation	
Maximum humidification/dehumidification gradient:	0.15%/minute	
Air velocity:	from 0.1 to 10 m/s	

Table 3
Characteristics of the DPE 240.

Measurement range	−2000 ÷ 2000 W/m^2
Sensing element	Termopila
Operating temperature	−30 ÷ 70°C
Sensitivity	64,4 mV/(W/m^2)
Uncertainty	5% v.l.
Response time	4 min
Temperature dependence	< 0.1%/°C

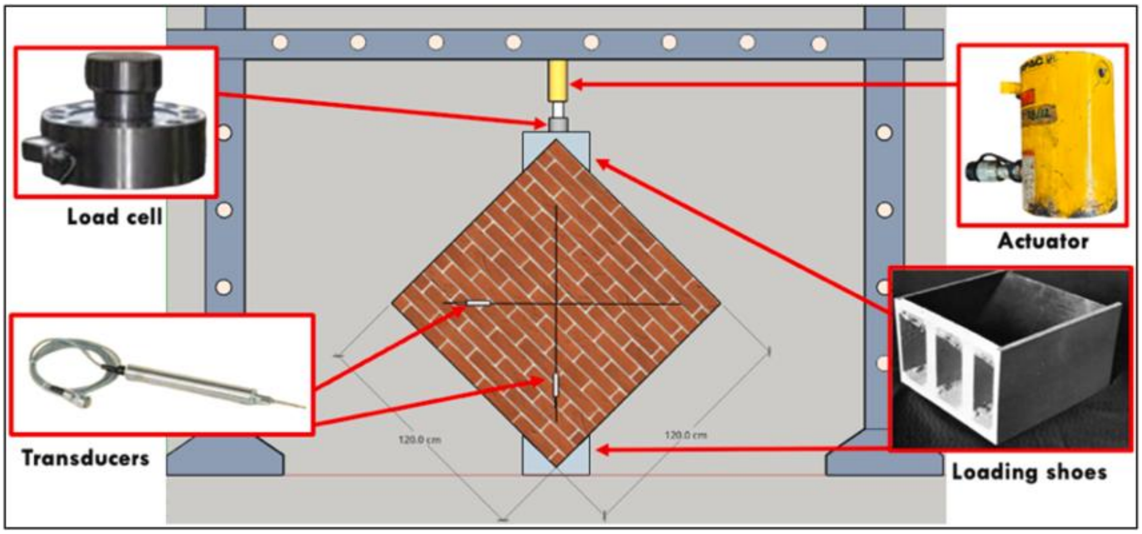

Fig. 19. Test setup and instrumentation layout showing the position of the load cell and displacement transducers used to measure diagonal shortening and elongation.

Fig. 20. Masonry wall: Specimen-60TRMTL3 for test.

specimens in accordance with ASTM E519/E519M − 22 [55].

2.3.3. Statistical analysis

To further quantify the experimental variability and assess whether the structural response was significantly affected by the investigated retrofit configuration, a statistical analysis was performed on the individual collapse-load measurements. A one-way analysis of variance (ANOVA) was adopted considering the wall configuration (NR, TL, TRM, TRMTL, TRMD, and TRMTLD) as the independent factor and the collapse load as the response variable. Statistical significance was assessed at a significance level of $\alpha = 0.05$. The assumptions underlying the ANOVA were checked through the Shapiro–Wilk test applied to the residuals and Levene's test for homogeneity of variances. In addition, the coefficient of variation (CoV) was calculated for each configuration to quantify

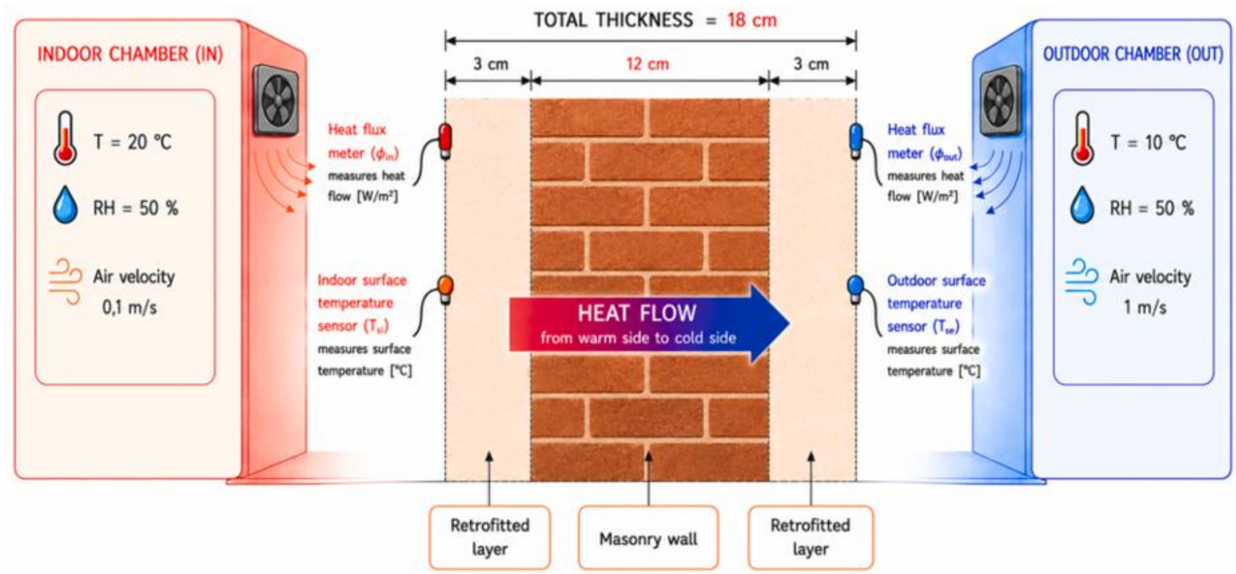

Fig. 21. Climate chamber: Masonry wall specimens testing.

specimen-to-specimen variability. The magnitude of the configuration effect was evaluated through the omega-squared (ω^2) effect-size estimator.

3. Results and discussion

All un-strengthened and retrofitted/upgraded masonry (60 cm × 60 cm) wall specimens were first subjected to thermal conductance tests, and thereafter, all these were subjected to diagonal compression (shear) tests.

3.1. Thermal test results

The tests were carried out by setting a temperature difference (ΔT) of 10°C between the two chambers, with a relative humidity of 50% in both, and air velocities of 0.1 m/s for the IN chamber and 1 m/s for the OUT chamber, respectively (Fig. 21).

The datalogger was set with a sampling frequency of 10 min. A sufficient time was allowed to reach steady-state conditions, in any case never less than 72 h. The steady-state condition was considered achieved in the absence of significant trends (increasing or decreasing) in the progressive average of the heat flux, and when its maximum fluctuation over the last 48 h remained within the instrument uncertainty:

$$max\left(\frac{1}{n}\sum_{1}^{n}\varphi\right)_{last\ 24h} - min\left(\frac{1}{n}\sum_{1}^{n}\varphi\right)_{last\ 24h} < U(\varphi) \tag{1}$$

The total thermal conductance of the wall was determined, in accordance with UNI EN ISO 9869-1 [58], as the ratio between the progressive average values of the heat flux and the difference in surface temperatures:

$$C = \frac{\frac{1}{n}\sum_{1}^{n}\varphi}{\frac{1}{n}\sum_{1}^{n}(T_{si} - T_{se})} \tag{2}$$

where:

- C is the total thermal conductance [W/m^{2}K];
- φ is the heat flux measured by the heat flux meter [W/m^2];
- T_{si} and T_{se} are the internal and external surface temperatures, respectively [°C].

The thermal resistance (R_M) of the different retrofitting layers forming the plaster of the generic Specimen X was obtained by the difference between the total resistance of Specimen X and the total resistance of the Reference Specimen without plaster.

The following Table 4 summarizes the results obtained for the un-strengthened and retrofitted masonry wall specimens tested in the Climate chamber. Column 2 reports the total thermal transmittance (U) of the wall; column 3 reports the total resistance of the wall ($R_{Wall\text{-}Total}$), and finally, column 4 reports the resistance ($R_{Retrofitting\ layer}$) of the individual retrofitted layer, obtained as half the difference between the resistance values Ri of the ith wall and the value R_1 of the first wall without retrofitting layers.

The total thermal transmittance (W/m^{2}K) of the un-strengthened and retrofitted/upgraded masonry wall can be calculated using (Fig. 22) the equation below:

$$U = \frac{1}{R_{in} + R_{Wall-Total} + R_{out}}\ (\mathrm{W}\ /\ \mathrm{m^2K}) \tag{3}$$

In, R_{in} is the indoor resistance (equal to 0.04 m^{2}K/W, the value provided in UNI EN 6946:2018 [73]), $R_{Wall\text{-}Total}$ is the total resistance of the masonry wall (without and with retrofitting layers, for the respective values see Table 4), R_{out} is the indoor resistance (equal to 0.13 m^{2}K/W, the value provided in UNI EN 6946:2018 [73]).

It should be noted that the thermal results reported in Table 4 refer to one wall specimen for each configuration; therefore, specimen-to-specimen variability cannot be statistically quantified. The uncertainty of the reported thermal measurements is governed by the measurement system, with the heat-flux sensor characterized by an uncertainty of approximately ±5% of the measured value.

Table 4
Thermal performance of the masonry walls tested in the Climate chamber.

Masonry wall specimens	Thermal transmittance masonry wall (U)	Thermal resistance of the retrofitted masonry wall ($R_{Wall\text{-}Total}$)	Total thermal resistance contribution of each retrofitting layer ($R_{Retrofitting\ layer}$)
	W/m^{2}K	m^{2}K/W	m^{2}K/W
60 NR	2.8563	0.1801	---
60 TL	2.4685	0.2351	0.0275
60TRM	2.4079	0.2453	0.0326
60TRMTL	2.0713	0.3128	0.0664
60TRMD	2.2894	0.2668	0.0434
60 TRMTLD	2.2292	0.2786	0.0493

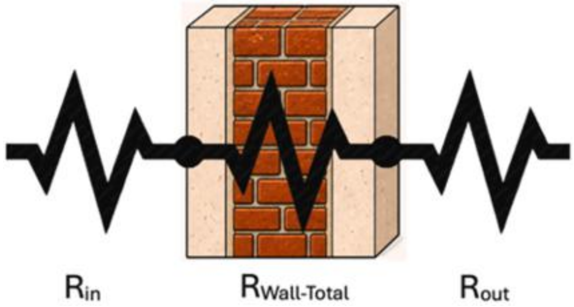

Fig. 22. Thermal resistances.

Accordingly, differences between configurations of the same order of magnitude should be interpreted with caution.

When all retrofitting combinations are considered, the overall increment in thermal resistance due to the addition of the retrofitting layers on both sides of the masonry walls is found to be between 0.055 m^2K/W and 0.1327 m^2K/W. Below we comment the thermal performance of each type of upgrading combination:

1. 60 TL, in this case the masonry wall was retrofitted with only Thermal Layers (NHL5, 30% recycled sand, 70% natural sand, and 1% of sheep wool fiber, the improvement is about 30,54%.
2. 60TRM, in which the masonry wall was retrofitted with TRM system consisting of flax fiber net, NHL5, 30% recycled sand, 70% natural sand, the improvement is about 36,20%.
3. 60TRMTL, in this case the masonry wall was retrofitted with TRM system consisting of flax fiber net, NHL5, 30% recycled sand, 70% natural sand, and 1% sheep wool fiber; the improvement is about 73,68%.
4. 60TRMD, here the masonry wall was retrofitted with TRM system consisting of flax fiber net, NHL5, 30% recycled sand, 70% natural sand, and a diaton, and the improvement results about 48,14%.
5. 60TRMTLD, the masonry wall was retrofitted with TRM system package consisting of flax fiber net, NHL5, 30% recycled sand, 70% natural sand, 1% sheep wool fiber, and a diaton; in this case the improvement is about 54,69%.

These improvements are attributed to the use of natural fibers (sheep wool fiber composite mortar layer, jute fiber diaton, and flax fiber net), especially the composite mortar and the layered structure of the retrofitting system, which helps in disrupting the heat flow, therefore reducing the thermal conductance values of the upgraded masonry walls.

3.2. *Structural test results of 60 cm × 60 cm wall specimens*

During walls preparation, mortar collected randomly from the construction site was used to prepare the prism samples, to evaluate the mechanical properties, and to understand its performance under real working conditions. More details about the statistical description of the test are present in Table 5. Further, these values were compared with the samples prepared in laboratory standard conditions (see, Fig. 23).

It is quite evident that samples prepared on-site exhibited lower strengths (flexural and compressive) when compared with the similar type of samples prepared in the lab. This variation depends on the fact that wall specimens were constructed during summer in open air. Therefore, water to cement ratio resulted relatively higher than usual because some extra water was continuously added by the workers to keep the mortar mixture workable.

Fig. 24 presents the un-strengthened 60NR3 masonry wall specimen before and after diagonal compression (shear) tests. In this case, all un-strengthened specimens completely collapsed after reaching the maximum peak load, ranging from 85.54 kN to 90.13 kN. Fig. 25 describes the failure of 60TL2 and 60TRM3 specimens after testing. Both specimens exhibited major diagonal cracks in the direction of the applied load, originating near the center region and propagating toward the edges. The observed crack patterns and material spalling indicate progressive shear and tensile stress interaction during failure. Fig. 26 illustrates specimens 60TRM1 and 60TRM2 after failure. The failed specimen showed a quasi-vertical crack extending through the panel. Notably, for 60TRM1, multiple

Table 5
Mechanical properties of the mortar, used to build the masonry wall, collected from the construction site.

	N° sample	Compression Strength		Flexural strength		Flexural strain		Flexural Modulus		Moment of inertia		Strain energy	
		Rc	CoV	fc	CoV	ε	CoV	E	CoV	I	CoV		CoV
		MPa	%	MPa	%		%	MPa	%	mm4	%	kN.mm	%
NHL(5F)100NS -Day1	6	3.43	6.88	0.76	21.58	0.023	3.71	33.52	19.01	224374.16	4.13	0.099	22.14
NHL(5F)100NS -Day2	6	3.45	4.83	0.88	6.77	0.023	7.77	37.63	9.02	228684.58	1.75	0.179	8.89

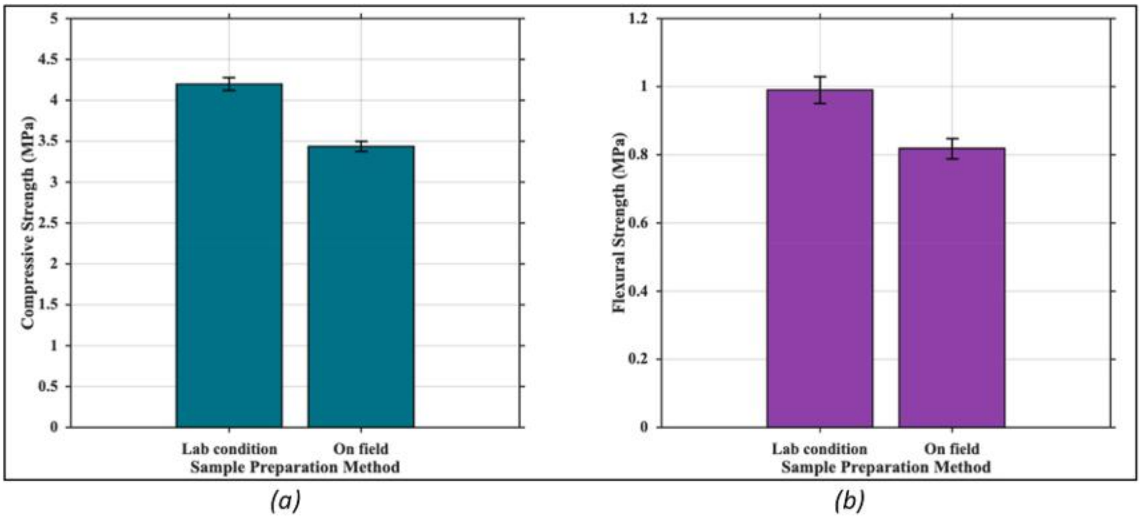

Fig. 23. Mechanical test results of samples prepared: (a) in the laboratory, and (b) on the construction site.

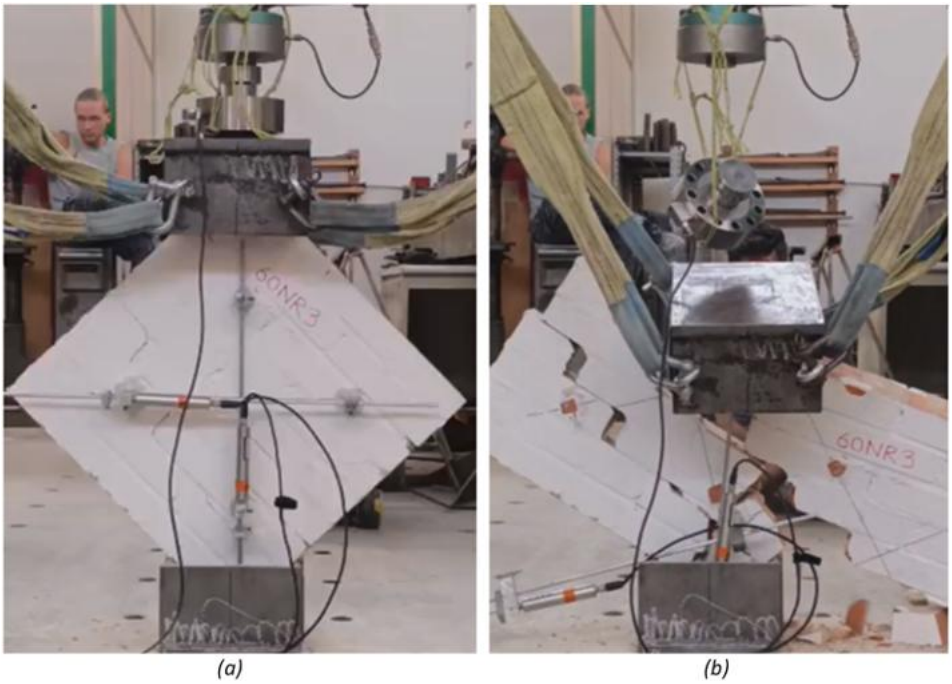

Fig. 24. Diagonal tension (shear) test: 60NR (a) before and (b) after the test.

cracks are visible and distributed.

Fig. 27 shows specimen 60TRMTL2 after testing. The specimen experienced extensive cracking along the central region with visible separation and deformation of the panel surface.

The structural properties have been calculated following the ASTM E519/E519M [55] standard.

The shear stress of the wall specimens has been calculated using the following equation:

$$S_s = \frac{0.707P}{A_n} \tag{3}$$

Where, S_S = Shear stress on the net area (MPa), P = applied load (N), and A_n = net area of the specimen.

Conversely, A_n is calculated as follows:

(a) (b)

Fig. 25. Diagonal compression (shear) test: (a) 60TL2, and (b) 60TRM3 after the test.

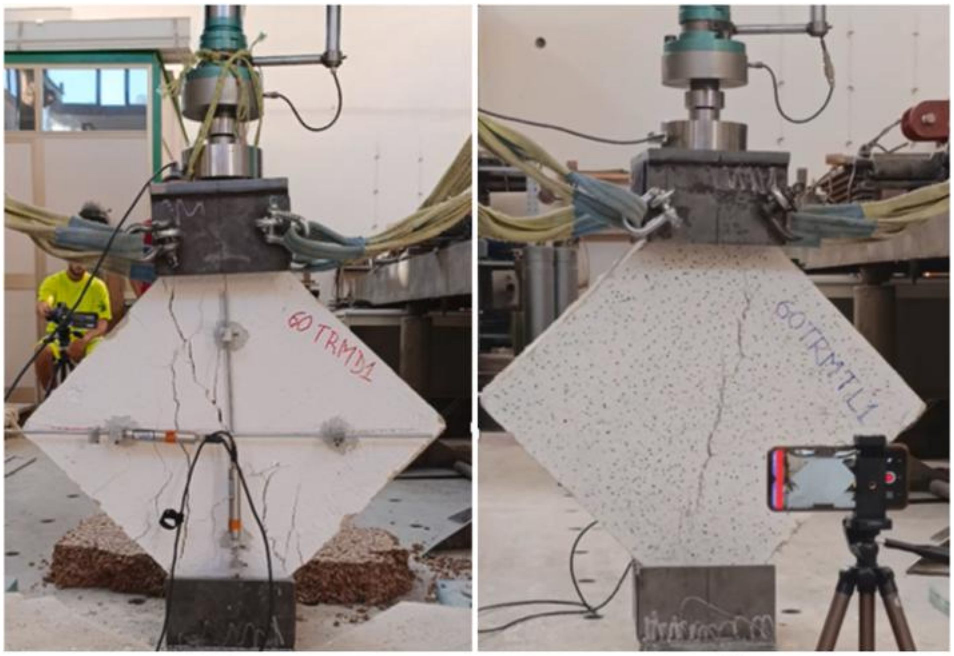

(a) (b)

Fig. 26. Diagonal compression (shear) test: (a) 60TRMD1, and (b) 60TRMTL1 after the test.

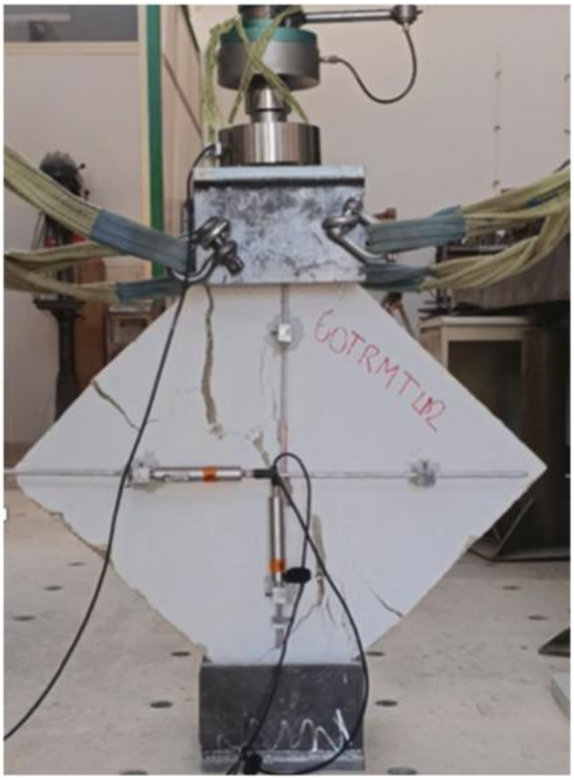

Fig. 27. Diagonal tension (shear) test: 60TRMTLD2 after the test.

$$A_n = \left(\frac{W + h}{2}\right) tn \tag{4}$$

where, W = width of the specimen (mm), h = height of the specimen (mm), t = total thickness of the specimen (mm), and n = percentage of gross area of the unit that is solid, expressed as a decimal.

The shear strain has been calculated using the following equation:

$$\gamma = \frac{\Delta V + \Delta H}{g} \tag{5}$$

where, γ = shearing strain, ΔV = vertical shortening (mm), ΔH = horizontal extension (mm), g = vertical gauge length (mm), please note that ΔH is based on the same gage length as for ΔV.

Moreover the modulus of rigidity G (MPa) has been calculated using the following equation:

$$G = \frac{S_s}{\gamma} \tag{6}$$

Table 6 presents the load-bearing capacities of the un-strengthened and retrofitted masonry walls.

The graphs presented in Fig. 28 show the stress–strain behavior of 60 cm × 60 cm masonry wall specimens under diagonal compression test.

The blue curves represent the average compressive stress, while the red curves represent the average tensile stress. The initial linear portion of the curves indicates elastic behavior, followed by peak stress and a softening region caused by cracking and material failure. The shaded areas represent the standard deviation among the three tests for each kind of panel.

To complement the experimental comparison and quantify the influence of specimen-to-specimen variability, a one-way ANOVA was performed on the collapse-load results. The analysis showed a statistically significant effect of the retrofit configuration on the structural response ($F = 3.87$, $p = 0.029$). The corresponding effect size was $\omega^2 = 0.458$, indicating that the differences among the investigated configurations account for a substantial proportion of the observed experimental variability. The assumptions of the analysis were also checked: Levene's test did not indicate significant heterogeneity of variances ($p = 0.534$), while the Shapiro–Wilk test applied to the residuals did not indicate a significant deviation from normality ($p = 0.354$). The coefficients of variation of the collapse load were 14.4%, 15.0%, 7.0%, 8.3%, 1.7%, and 27.9% for NR, TL, TRM, TRMTL, TRMD, and TRMTLD, respectively. Five of the six investigated configurations therefore showed coefficients of variation not exceeding approximately 15%, while the dispersion

Table 6
Load-bearing capacities.

	P_{max}	$Ss_{ultimate}$	$Ss_{avg.}$	$\gamma_{avg.}$	$G_{avg.}$
	kN	MPa	MPa		MPa
60NR	90.13	0.8790	0.5007	1.06E-04	6794.32
60 TL	134.43	1.2827	0.7819	2.76E-04	8350.30
60TRM	105.91	0.8964	0.5868	9.81E-04	1875.98
60TRMTL	125.61	1.2260	0.8962	5.82E-04	4105.74
60TRMD	143.59	1.1172	0.7212	2.29E-04	5785.31
60TRMTLD	123.22	0.9341	0.7179	6.62E-04	2929.19

observed for the remaining configuration reflects the intrinsic variability associated with destructive testing of masonry assemblages. Together with the standard-deviation bands reported in Fig. 27, these statistical results support that the differences observed among the investigated configurations cannot be attributed solely to random specimen variability.

The 60NR specimens (in Fig. 28a), the unreinforced reference walls, notably, have shown the lowest strength and stiffness. 60NR wall specimens have exhibited brittle behavior with complete collapse.

The 60 TL specimens (in Fig. 28b) with sheep-wool fiber composite mortar layers on both faces showed the highest strength and stiffness among all samples. The steep stress–strain curve indicates efficient load transfer capacity, although the lower strain range suggests a more brittle response after peak load. The maximum load withstood by 60TL3 was found to be about 49.15% higher when compared with the reference specimen.

In the case of 60TRM wall specimens (in Fig. 28c), the application of net, helps to enhance the effectiveness of crack control as well as the stress distribution, giving the wall better ductility and high strength when compared with the wall without reinforcement. The maximum load withstood by 60TRM2 was found to be about 17.51% higher than that of the reference specimen.

The 60TRMTL specimens (in Fig. 28d) combine flax net reinforcement with sheep-wool fiber composite mortar. This system enhances rigidity and strength and improves the bond between the retrofitted layer and the wall. But due to its lower strain capacity compared to TRM, ductility is compromised, and cracking becomes more localized post-peak load. The maximum load withstood by 60TRMTL3 was found to be about 39.37% higher with respect to the reference specimen.

The 60TRMD specimens (in Fig. 28e), were reinforced with flax nets and diatons, whose application enhanced the connection between both faces of the wall and improved structural integrity. As a result, this specimen shows high strength, improved stiffness, and better crack resistance under diagonal compression. The maximum load withstood by 60TRMD2 was about 59.32% higher compared with the reference specimen.

The 60TRMTLD specimens (in Fig. 28f) retrofitted with a complete TRM package (flax nets, sheep-wool fiber composite mortar, and diaton) demonstrated a balanced behavior, with good strength and higher ductility. The gradual stress reduction after peak load indicates stable crack propagation and high energy-absorption capacity, making it effective at resisting seismic-type loading. The maximum load withstood by 60TRMTLD3 was approximately 36.72% higher than that of the reference specimen. Table 7 compares the diagonal compression test results obtained in this study with those reported in previous investigations on TRM-strengthened masonry walls. Although direct quantitative comparisons are complicated by differences in masonry typology, specimen dimensions, textile reinforcement, and test configurations, several observations can be made. Firstly, the strengthening effectiveness achieved by the proposed NFTRM systems is comparable to that reported for conventional TRM solutions reinforced with basalt, carbon, or AR-glass fibers. Secondly, unlike the literature studies, which focus exclusively on structural strengthening, the proposed retrofit strategy simultaneously improves structural and thermal performance through the combined use of flax textiles, sheep-wool insulating mortar, jute-fiber diatons, and recycled aggregates. Finally, the adoption of bio-based and recycled materials significantly enhances the sustainability of the intervention while maintaining competitive mechanical performance, demonstrating the feasibility of integrated thermo-structural retrofitting solutions for existing masonry buildings.

3.3. Discussion on integrated results

The relative structural and thermal performance of the different masonry wall configurations shown in Fig. 29 indicates that the investigated retrofit solutions provide different levels of improvement compared with the unreinforced wall (60NR), which is taken as the reference condition (relative value = 1.00).

However, none of these configurations gives optimum structural and thermal performance simultaneously. The 60TRMD configuration shows the best relative load-bearing capacity of 1.59 (59% better than 60NR), whereas 60TRMTL configuration shows the best thermal resistance of 1.74 (74% better than 60NR).

To further quantify the contribution of the individual components, a configuration-based sensitivity analysis was performed using paired comparisons between wall systems differing by one retrofit component, see Table 8.

The percentage variations were calculated using the maximum load $P_{\max}$ and total wall thermal resistance reported in Table 6 andTable 4, respectively. Adding the flax-based TRM component to the thermal-layer configuration (TL→TRMTL) resulted in a 6.6% decrease in $P_{\max}$ and a 33.1% increase in thermal resistance. The addition of sheep wool to the TRM system (TRM→TRMTL) increased $P_{\max}$ by 18.6% and thermal resistance by 27.5%, whereas its addition to the diaton-enhanced system (TRMD→TRMTLD) resulted in a 14.2% decrease in $P_{\max}$ but a further 4.4% increase in thermal resistance. The strongest positive structural contribution among the

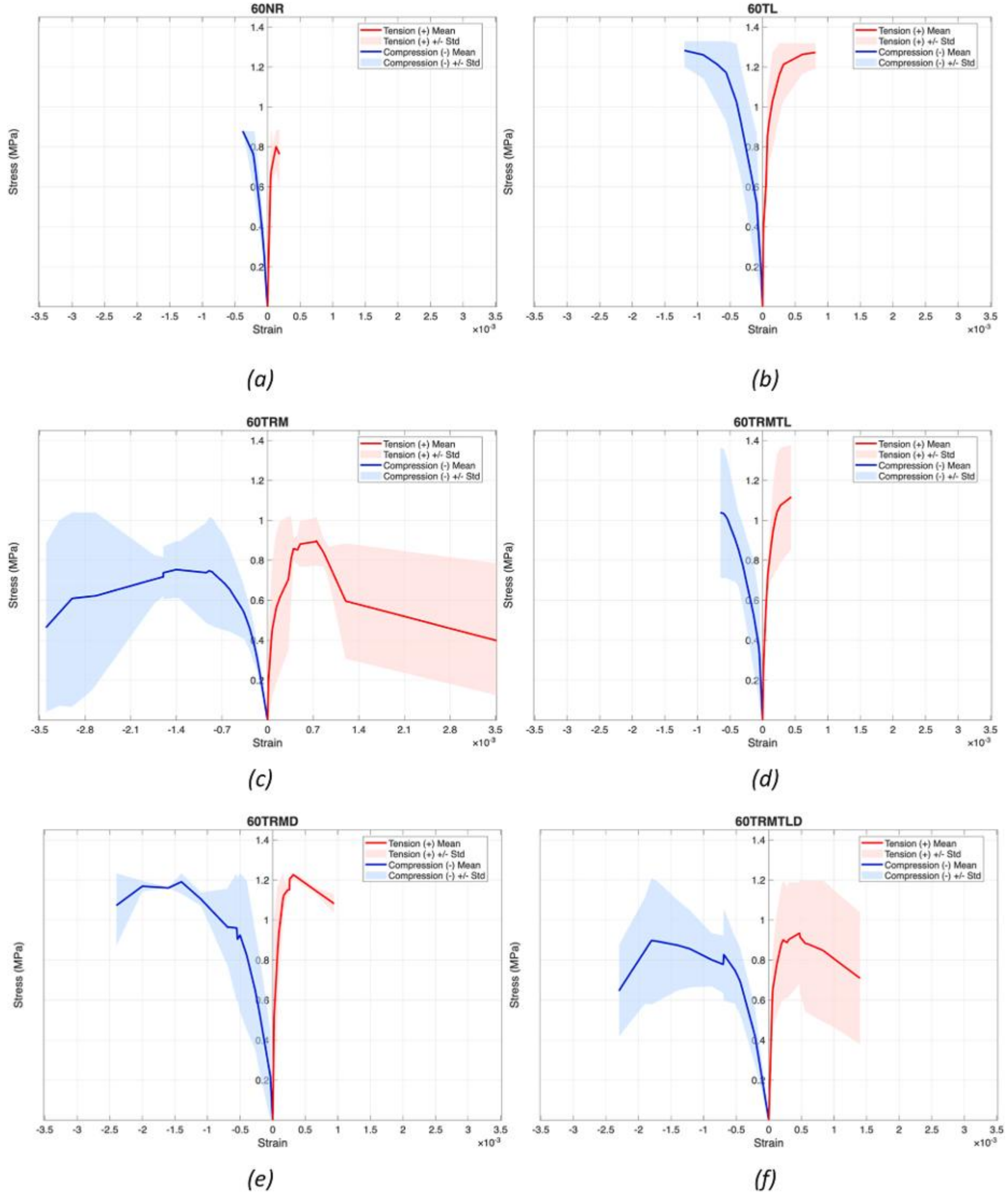

Fig. 28. Stress–strain curves of (a) 60NR, (b) 60 TL, (c) 60TRM, (d) 60TRMTL, (e) 60TRMD, and (f) 60TRMTLD. Solid curves represent the average experimental response, while shaded regions indicate the experimental variability expressed as standard deviation.

directly comparable configurations was obtained by adding jute diatons to TRM (TRM→TRMD), which increased P_{max} by 35.6%, together with an 8.8% increase in thermal resistance. In contrast, adding diatons to TRMTL (TRMTL→TRMTLD) produced changes of −1.9% and −10.9% in P_{max} and thermal resistance, respectively.

These comparisons demonstrate that the contribution of the retrofit components is not simply additive but depends on their

Table 7
Comparison with various diagonal tests campaigns.

	Retrofitting Strategy	Specimen nomenclature	Wall surface area	Structural properties	Reference sample	Test type
This research	Thermal layer Structural Integrated (Structural and thermal)	TL TRM TRMTL TRMD TRMTLD	60 cm × 60 cm	See, Table 6		Diagonal shear test
Ozen et al. (2024) [23]	Structural	Basal fiber TRM	78.5 cm × 78.5 cm	Max load = 60.69 – 68.93 (kN) Shear stress = 1.05-1.19 (MPa)	Ultimate load = 33.86 (kN) Max Shear stress = 0.59 (MPa)	Diagonal shear test
	Structural	Carbon fiber TRM		Max load = 63.81-83.39 (kN) Shear stress = 1.10-1.44 (MPa)		Diagonal shear test
Marcari et al. (2017) [74]	Structural	Single-Side Basalt fiber TRM Double-Side Basalt fiber TRM	100 cm × 100 cm	Max Shear Stress = 0.52 MPa (avg.) Max Shear Stress = 0.62 (MPa) (avg.)	Max Shear stress = 0.39 (MPa)	Diagonal shear test Diagonal shear test
Ungureanu et al. (2021) [75]	Structural	Single-side carbon fiber TRM	120 cm × 120 cm	Ultimate load = 43.02 (kN) Max Shear stress = 0.114 MPa (avg.)	Ultimate load = 25.43 (kN) Max Shear stress = 0.043 (MPa)	Diagonal shear test
		Double-side carbon fiber TRM		Ultimate load = 58.70 (kN) – 59.36 (kN) Max Shear stress = 0.137 (MPa) - 167 MPa (avg.)		Diagonal shear test
Shabdin et al. (2018) [76]	Structural	Single-side AR glass fiber TRM	120 cm × 120 cm	Max load = 211 (kN) Max. Shear stress = 1.54 (MPa)	Ultimate load = 5.4 (kN)	Diagonal shear test
		Single-side AR glass fiber TRM		Max load = 287 kN – 355 (kN) Max. Shear stress = 2.00 (MPa) – 2.33 (MPa)		Diagonal shear test
Gkournelos et al. (2020) [77]	Structural	Double-side AR glass fiber TRM	6 cm × 86 cm	Max. Shear stress = 1.63 (MPa)	Max Shear stress = 0.78 (MPa)	Diagonal shear test

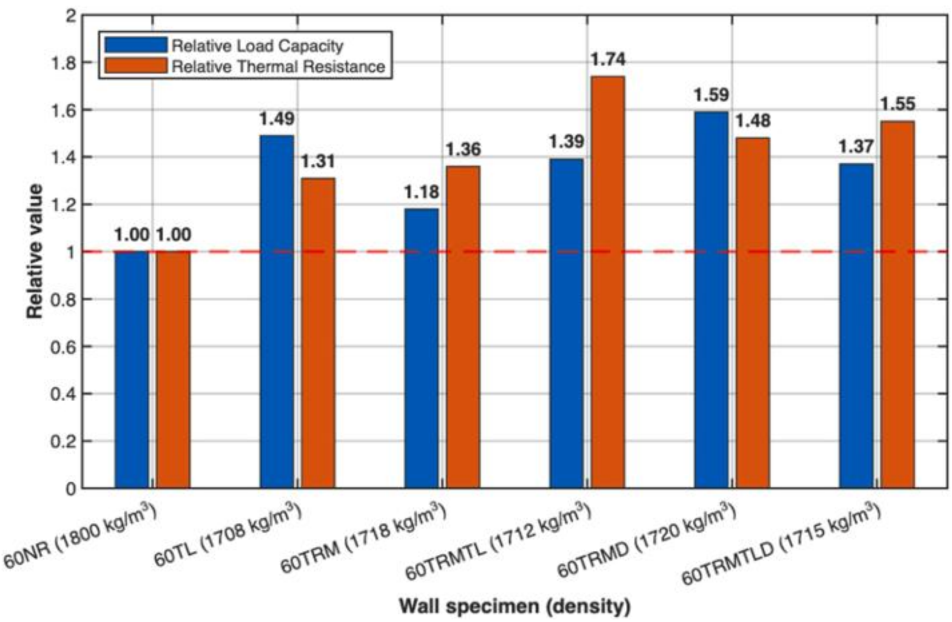

Fig. 29. Relative structural and thermal performance.

Table 8
Integrated analysis on the role of each layer of the retrofitting system.

Component investigated	Paired configurations	Δ P_{max}	Δ $R_{Thermal}$	Interpretation
Flax textile	TL → TRMTL	−6.6%	+33.10%	Effect is not expressed simply through peak load; textile modifies the composite response and crack redistribution.
Sheep wool	TRM → TRMTL	+18.60%	+27.50%	Strong positive thermo-structural contribution in the absence of diatons.
Sheep wool	TRMD → TRMTLD	−14.2%	+4.40%	Thermal contribution remains positive, while structural effect becomes interaction dependent.
Jute diaton	TRM → TRMD	+35.60%	+8.80%	Largest positive structural increment among the directly comparable configurations.
Jute diaton	TRMTL → TRMTLD	−1.9%	−10.9%	Effect changes when combined with the thermal layer, demonstrating non-additive interaction.
Recycled sand	Preliminary mortar campaign	—	—	Cannot be isolated at wall level because 30% RS is kept constant; its contribution was assessed separately during mortar selection

interaction within the composite system. In particular, the jute diatons provide the largest directly observed structural increment when combined with TRM, whereas sheep wool provides the most consistent contribution to thermal performance. The flax textile primarily acts as distributed tensile reinforcement, contributing to stress redistribution and crack control, while its contribution cannot be described solely through changes in peak load. Recycled sand cannot be isolated through paired wall comparisons because the selected 30% replacement ratio was maintained in the retrofit mortar mixtures. Its influence was therefore assessed separately during the preliminary mortar optimization campaign, where 30% RS provided the most favorable balance between mechanical and thermal performance among the investigated replacement levels.

Furthermore, to quantitatively evaluate the combined structural and thermal response, an Integrated Performance Index (IPI) has been introduced here, by assigning equal importance (50% each) to the two performance indicators, structural and thermal performances, respectively.

First, the structural performance of each configuration was normalized with respect to the collapse load of the reference wall (60NR) as:

$$R_{Load,i} = \frac{P_i}{P_{60NR}} \tag{7}$$

where P_i is the collapse load of the wall configuration, and P_{60NR} is the collapse load of the reference wall.

Similarly, the relative thermal performance was calculated by normalizing the thermal resistance with respect to the reference wall:

$$R_{Thermal,i} = \frac{R_i}{R_{60NR}} \tag{8}$$

where R_i is the thermal resistance of the wall configuration, and R_{60NR} is that of the reference wall.

Thus, the IPI represents the equally weighted average of the normalized structural and thermal performances, with corresponding to the performance of the reference 60NR wall. **IPI** has been subsequently determined as the equally weighted arithmetic mean of the two normalized performance indicators, assuming equal weighting (50% structural + 50% thermal):

$$IPI_i = \frac{R_{Load,i} + R_{Thermal,i}}{2} \tag{9}$$

Accordingly, an IPI of 1.00 represents the overall performance of the reference 60NR wall, while values greater than 1.00 indicate an integrated improvement (Table 9).

Notably, 60TRMTL exhibited the highest integrated performance, with an IPI of 1.565, calculated as ((1.39 + 1.74)/2 = 1.565), followed closely by 60TRMD (IPI = 1.535) and 60TRMTLD (IPI = 1.460).

Therefore, although 60TRMTL does not provide the highest structural capacity, its combination of a relative load capacity of 1.39 and the highest relative thermal resistance of 1.74 results in the most favorable overall performance under the adopted equal-weight criterion. These results demonstrate that the combined retrofit systems can simultaneously enhance the structural and thermal performance of masonry walls, although the identification of the optimum configuration depends on the relative weighting assigned to structural and thermal requirements.

Table 9
Integrated (Structural + thermal) performance evaluation.

Rank of performance	Wall sample	Integrated performance index (IPI)	Improvement vs. 60NR
1	60TRMTL	1.57	56.50%
2	60TRMD	1.54	53.50%
3	60TRMTLD	1.46	46.00%
4	60 TL	1.40	40.00%
5	60TRM	1.27	27.00%
6	60NR	1.00	Reference

Table 10
Comparison between several integrated retrofitting/upgrading strategies.

	Integrated (structural and thermal) Retrofitting	Specimen retrofitting strategies	Wall surface area	Thermal properties: Reference sample	Thermal properties: Retrofitted sample	Structural properties: Reference sample	Structural properties: Retrofitted sample
This research	Natural fiber	Flax fiber TRM + jute fiber diatons	60 cm × 60 cm	See, Table 4		See, Table 6	
Stochino et al. (2025) [51]	Natural fiber	Jute fiber TRM system package (jute net + jute diatons + jute fiber composite mortar)	100 cm × 100 cm	1.77 (W/m^{2}K)	1.34 (W/m^{2}K)	Load bearing capacity (in plane): 37.7 (kN)	Load bearing capacity (in plane): 236 (kN)
Stochino et al. (2025) [78]	Man-made fiber	Steel or Basalt fiber TRM with diatons + Lime based thermal insulation mortar	120 cm × 100 cm	Clay brick = 1.79 (W/m^{2}K); Concrete brick = 2.00 (W/m^{2}K)	Clay brick = 0.99 (W/m^{2}K) to 1.03 (W/m^{2}K); Concrete brick = 1.30 (W/m^{2}K) to 1.37 (W/m^{2}K)	Load bearing capacity (in plane): Clay brick = 72 (kN) and 134 (kN); Concrete brick = 141 (KN) and 167 (kN)	Load bearing capacity (in plane): Clay brick = 150 (kN) to 200 (KN); Concrete brick = 151 (kN) to 212 (KN)
Furtado et al. (20203) [79]	Man-made fiber	Glass fiber TRM + Expanded Polystyrene	420 cm × 230 cm	1.75 (W/m^{2}K)	0.30 (W/m^{2}K) to 0.40 (W/m^{2}K)	Load bearing capacity (out of plane): 45 (kN)	Load bearing capacity (out of plane): 65 (kN) to 100 (kN)
Facconi et al. (2021) [80]	Man-made fiber	Steel fiber TRM on full scale building) + Aerogel, light wood fiber, and heavy wood fiber (analytical and numerical).	670.7 cm × 575.0 cm	1.04 (W/m^{2}K)	Analytical: 0.242 (W/m^{2}K) to 0.335 (W/m^{2}K); Numerical 0.246 (W/m^{2}K) to 0.336 (W/m^{2}K)	Load bearing: 180 (kN)	Load bearing: 605 (kN)
Longo et al. (2021) [81]	Man-made fiber	Glass fiber TRM + Hydraulic lime and GeoPolymer lime	51 cm × 51 cm	2.08 (W/m^{2}K)	1.051 (W/m^{2}K) to 1.56 (W/m^{2}K)	Load bearing: 46,18	79.71 (kN) to 107.25 (kN)
Gkournelos et al. (2020) [77]	Man-made fiber	Glass fiber TRM + Expanded Polystyrene (EPS) insulation panel	86 cm × 86 cm	NO test has been performed, considered improvement in insulation property due to the application of EPS		Load bearing capacity (out of plane): 1.60 (kN)	Load bearing capacity (out of plane): 25.3 (kN)
Gkournelos et al. (2023) [82]	Man-made fiber	Glass fiber TRM + Expanded Polystyrene (EPS) insulation panel	45 cm × 45 cm	NO test has been performed, considered improvement in insulation property due to the application of EPS		Load bearing capacity (out of plane): 47.4 (kN)	Load bearing capacity (out of plane): 69.2 (kN)
Karlos et al. (2020)	Man-made fiber	Glass fiber TRM + Expanded Polystyrene (EPS) insulation panel	150 cm × 40 cm	NO test has been performed, considered improvement in insulation property due to the application of EPS		Three-point bending tests: Peak loads Reference wall 3.42 (kN)	Three-point bending tests: Peak loads 9.28 (kN) to 20.26 (kN);
Triantafillou et al. (2018)	Man-made fiber	Glass fiber TRM + Expanded Polystyrene (EPS) insulation panel		NO test has been performed, considered improvement in insulation property due to the application of EPS		Three point bending test: 3.42 (kN)	Three point bending test: 8.06 (kN) to 20.26 (kN)
Triantafillou et al. (2018)	Man-made fiber	Glass fiber TRM + Expanded Polystyrene (EPS) insulation panel		NO test has been performed, considered improvement in insulation property due to the application of EPS		Peak loads 19.9 (kN) for type-A, 20 (kN) for type-B, and 12.2 (kN) for type-C	1.5 (kN) - 37.5 (kN) for Type-A, 29.2–37.1 (kN) for type-B and 24.3 (kN) – 36.8 (kN) for type-C,

While Table 10 summarizes the main integrated thermo-structural retrofitting strategies reported in the literature, including both natural-fiber- and man-made-fiber-based systems. The comparison considers wall dimensions, thermal performance, structural performance, and the corresponding retrofit configurations. Most previous studies have focused on combining conventional TRM systems reinforced with steel, glass, basalt, or carbon fibers with external thermal insulation materials such as expanded polystyrene (EPS), aerogel, wood-fiber panels, or lime-based insulating mortars. In contrast, only a limited number of investigations have fully explored bio-based integrated retrofitting solutions. The proposed NFTRM system, combining flax fiber textiles, sheep-wool insulating mortars, jute-fiber diatons, and recycled aggregates, represents one of the few examples of fully natural-fiber integrated retrofit strategy. Despite the use of sustainable and low-impact materials, the thermo-structural improvements achieved in this study are comparable with those reported for conventional integrated retrofit systems, demonstrating the potential of bio-based solutions as viable alternatives for the sustainable upgrading of existing masonry buildings.

The comparison reported in Table 10 highlights a clear trend in recent research towards integrated retrofit solutions capable of simultaneously improving energy efficiency and structural safety. However, the most of the available systems rely on synthetic fibers and petroleum-based insulation materials. Conversely, the natural-fiber-based solutions proposed by Stochino et al. [44] and in the present study achieve substantial thermo-structural improvements while significantly enhancing sustainability and circularity. In particular, the use of flax fibers, sheep wool, jute diatons, and recycled aggregates reduces dependence on high-embodied-energy materials while maintaining competitive structural performance. These findings support the development of environmentally responsible retrofit strategies capable of addressing both seismic and energy-efficiency requirements within a single intervention.

4. Conclusion

This study investigated the thermo-structural performance of NFTRM systems developed for integrated retrofitting/upgrading of masonry walls. The proposed systems combined flax fiber textile nets, sheep wool fiber composite mortars, jute fiber diatons, and 30% recycled aggregates to simultaneously improve the structural and thermal behavior of masonry panels. Based on the experimental campaign, the following conclusions can be drawn:

- The use of natural fibers and recycled aggregates proved to be an effective and sustainable solution for integrated masonry retrofitting/upgrading applications.
- Among the investigated mortar mixtures, the replacement of natural sand with 30% recycled sand provided the best balance between mechanical and thermal properties, showing the highest flexural strength together with improved thermal insulation characteristics.
- All the retrofitting systems improved the thermal properties of the masonry wall compared to the reference unreinforced masonry wall. The TRMTL system has shown the greatest improvement, with thermal resistance increasing by approximately 73.68%.
- The inclusion of sheep wool fibers in the composite mortar contributed significantly to reducing thermal conductance by improving the insulating behavior of the retrofitting layers.
- The flax fiber TRM systems enhanced the structural response of the masonry walls under diagonal compression loading, improving crack distribution, delaying brittle collapse, and increasing the load-bearing capacity compared to the un-strengthened walls.
- The incorporation of jute fiber diatons improved the integrity of the retrofitted systems, contributing to better structural stability.
- The combined use of flax fiber net, sheep wool composite mortar, jute diatons, and recycled aggregates demonstrated that fully bio-based and recyclable materials can be successfully employed in integrated retrofitting strategies for masonry structures. Although a detailed LCA is beyond the scope of this study, the use of recycled aggregates and natural fibers is expected to reduce embodied environmental impacts compared with conventional TRM systems.

Overall, all tested NFTRM systems have demonstrated a promising sustainable retrofitting solution for existing masonry structures. It can be used for retrofitting existing and heritage buildings, as well as energy-inefficient ones. Future research will focus on durability, environmental exposure effects, and design and construction guidelines for NFTRMs.

Although the present experimental results demonstrate the potential of the proposed NFTRM systems for integrated thermo-structural retrofitting of masonry, the findings should not be interpreted as a complete validation for unrestricted field application.

Further investigations addressing long-term durability, environmental exposure and benefits, full-scale implementation, workmanship sensitivity, quality-control procedures, and additional structural loading conditions are required before widespread practical application can be recommended. In parallel, the development of dedicated standards and qualification procedures for NFTRM systems would be an important step toward reliable use in real engineering applications.

Notably, the use of natural fibers and recycled aggregates provides a promising pathway toward more sustainable retrofit solutions, the magnitude of the environmental benefit cannot be quantitatively established from the present experimental campaign alone**.** Quantification of these benefits is therefore reserved for the dedicated comparative environmental study currently under development.

The structural conclusions of the present study are therefore limited to the in-plane shear response investigated through diagonal compression tests and should not be directly generalized to cyclic in-plane loading, out-of-plane bending, flexural, impact, or other loading conditions. Dedicated experimental campaigns are required to assess the performance of the proposed NFTRM system under these additional structural actions before a comprehensive validation for engineering applications can be established.

CRediT authorship contribution statement

Arnas Majumder: Writing – review & editing, Writing – original draft, Visualization, Validation, Methodology, Investigation, Formal analysis, Data curation, Conceptualization. **Monica Valdes:** Writing – review & editing, Visualization, Validation, Software, Data curation. **Giovanna Concu:** Writing – review & editing, Visualization, Validation, Supervision, Conceptualization. **Andrea Frattolillo:** Writing – review & editing, Visualization, Validation, Supervision, Resources, Methodology. **Maria Francesca Sabbà:** Writing – review & editing, Visualization, Validation, Formal analysis. **Marco Pepe:** Writing – review & editing, Visualization, Validation, Resources, Project administration, Methodology, Conceptualization. **Flavio Stochino:** Writing – review & editing, Writing

– original draft, Visualization, Validation, Supervision, Resources, Project administration, Methodology, Funding acquisition, Conceptualization.

Declaration of competing interest

The authors declare that they have no known competing financial interests or personal relationships that could have appeared to influence the work reported in this paper.

Acknowledgement

The authors gratefully acknowledge the financial support provided by the PRIN PNRR 2022 project Integra TRM: Integrated Seismic and Thermal Upgrading of Existing Masonry Buildings through a Novel Sustainable Textile-Reinforced Mortar System (F53D23009850001). The authors wish to thank Brebey Srl for providing the Sardinian sheep-wool fibers used in this research.

Also, the authors would like to thank Theo, Sasha, and Aya for their relentless work and their enthusiasm through the whole experimental campaign.

Data availability

Data will be made available on request.

References

[1] U.N. Environment, Global Status Report for Buildings and Construction 2024/2025, UNEP - UN Environment Programme, 2025. https://www.unep.org/resources/report/global-status-report-buildings-and-construction-20242025. (Accessed 16 May 2026).
[2] P. Zhang, L. Chen, T. Wei, P. Huang, H. Wang, X. Chen, Multi-Hazard assessment of masonry buildings: a state-of-the-art review, Buildings 14 (2024), https://doi.org/10.3390/buildings14123711.
[3] T. Zhang, X. Li, W. Ning, Z. Hou, K. Li, X. Yang, Seismic performance of masonry walls retrofitted with a low-carbon and low-intervention sprayed ECC: experimental and analytical studies, J. Build. Eng. 125 (2026) 116152, https://doi.org/10.1016/j.jobe.2026.116152.
[4] J. Kubica, Development of masonry materials and structures from ancient times, through the present times and the future perspective, J. Build. Eng. 116 (2025) 114682, https://doi.org/10.1016/j.jobe.2025.114682.
[5] A. Majumder, F. Stochino, M. Valdes, G. Concu, M. Pepe, E. Martinelli, Sustainable masonry retrofitting and upgrading techniques: a review, Fibers 13 (2025) 68, https://doi.org/10.3390/fib13060068.
[6] E. Martinelli, F. Perri, C. Sguazzo, C. Faella, Cyclic shear-compression tests on masonry walls strengthened with alternative configurations of CFRP strips, Bull. Earthq. Eng. 14 (2016) 1695–1720, https://doi.org/10.1007/s10518-016-9895-6.
[7] D.A. Pohoryles, D.A. Bournas, F. Da Porto, A. Caprino, G. Santarsiero, T. Triantafillou, Integrated seismic and energy retrofitting of existing buildings: a state-of-the-art review, J. Build. Eng. 61 (2022) 105274, https://doi.org/10.1016/j.jobe.2022.105274.
[8] European Commission. Joint Research Centre, Integrated techniques for the seismic and energy renovation of buildings - Joint research centre, n.d, https://joint-research-centre.ec.europa.eu/projects-and-activities/integrated-techniques-seismic-and-energy-renovation-buildings_en. (Accessed 26 June 2026).
[9] L.S. Armando, J. Pereiro-Barceló, D. Foti, S. Ivorra, Detailed numerical micro-modelling of masonry TRM reinforcements, in: Y. Endo, T. Hanazato (Eds.), Structural Analysis of Historical Constructions, Springer Nature Switzerland, Cham, 2024, pp. 543–555, https://doi.org/10.1007/978-3-031-39450-8_45.
[10] A. La Scala, D. Foti, J. Pereiro-Barcelò, S. Ivorra, Numerical analysis of residual tensile properties and strain rate sensitivity of textile reinforced mortar interface behavior after thermal exposure, Arch. Civ. Mech. Eng. 26 (2026) 168, https://doi.org/10.1007/s43452-026-01538-x.
[11] Alper Ilki, Medine Ispir, Fundagul As, Cem Demir, Nahit Kumbasar, FRP retrofit of walls constructed with historical bricks, CCC2008, https://ishmii.org/wp-content/uploads/2010/07/frp-retrofit-of-walls.pdf, 2008.
[12] P. Narayanan, M. Deivanayagam, Retrofitting and rehabilitation of masonry structures using FRP composites, Mater. Today Proc. (2023), https://doi.org/10.1016/j.matpr.2023.05.096.
[13] X. Sun, P. Shi, H. Zhu, Z. Dong, B. Mu, C.K. Soh, Shear performance of brick masonry walls strengthened by deep structural repointing using FRP reinforcement, J. Build. Eng. 111 (2025) 113187, https://doi.org/10.1016/j.jobe.2025.113187.
[14] B. Luccioni, V.C. Rougier, In-plane retrofitting of masonry panels with fibre reinforced composite materials, Constr. Build. Mater. 25 (2011) 1772–1788, https://doi.org/10.1016/j.conbuildmat.2010.11.088.
[15] B. Abdulsalam, A.H. Ali, A. ElSafty, N. Elshafey, Behavior of GFRP strengthening masonry walls using glass fiber composite anchors, Structures 29 (2021) 1352–1361, https://doi.org/10.1016/j.istruc.2020.12.025.
[16] M. Hadzima-Nyarko, S. Čolak, B.Đ. Bulajić, N. Ademović, Assessment of selected models for FRP-retrofitted URM walls under In-Plane loads, Buildings 11 (2021), https://doi.org/10.3390/buildings11110559.
[17] H. Mahmood, J.M. Ingham, Diagonal compression testing of FRP-retrofitted unreinforced clay brick masonry wallettes, J. Compos. Construct. 15 (2011) 810–820, https://doi.org/10.1061/(ASCE)CC.1943-5614.0000209.
[18] T. Ozbakkaloglu, J.-F. Chen, S.T. Smith, J.-G. Dai, Applications of fiber reinforced polymer composites, Int. J. Polym. Sci. 2016 (2016), https://doi.org/10.1155/2016/5804145, 1–1.
[19] M.C. Yılmaz, A.A.E. Finner, Ö. Mercimek, Experimental investigation of out-of-plane behaviour of unreinforced masonry panels strengthened with TRM, Structures 65 (2024) 106665, https://doi.org/10.1016/j.istruc.2024.106665.
[20] Integrated TRM System for the Seismic Strengthening of Masonry Heritage | CONNECT | Project | Fact Sheet | H2020, CORDIS, European Commission, 2023, https://doi.org/10.3030/101038043.
[21] B. Torres, S. Ivorra, F. Javier Baeza, L. Estevan, B. Varona, Textile reinforced mortars (TRM) for repairing and retrofitting masonry walls subjected to in-plane cyclic loads. An experimental approach, Eng. Struct. 231 (2021) 111742, https://doi.org/10.1016/j.engstruct.2020.111742.
[22] F. Stochino, A. Majumder, A. Frattolillo, M. Valdes, M. Sassu, F. Mistretta, Structural and thermal performance of masonry walls: insights from TRM-based upgrading techniques, Structures 81 (2025) 110200, https://doi.org/10.1016/j.istruc.2025.110200.
[23] A. Özen, A. Çelik, S.T. Akkaya, K. Bıçakçıoğlu, Ö. Mercimek, M.C. Yılmaz, Y. Erbaş, Ö. Anıl, Experimental investigation of behavior of masonry wall under diagonal tension loading: strengthening with CFRP versus TRM, Structures 70 (2024) 107723, https://doi.org/10.1016/j.istruc.2024.107723.
[24] A. Cascardi, L.N. Koutas, S. De Santis, B. Ghiassi, F. Micelli, M.A. Aiello, T. Triantafillou, Textile-reinforced mortar (TRM) for retrofitting masonry structures: advantages, challenges and future potential, Mater. Struct. 59 (2026) 38, https://doi.org/10.1617/s11527-025-02891-8.
[25] O.G. Agossou, S. Amziane, Analysis of mechanical and thermal performance and environmental impact of flax-fiber-reinforced gypsum boards, Buildings 13 (2023), https://doi.org/10.3390/buildings13123098.

[26] A. Majumder, F. Stochino, A. Frattolillo, M. Valdes, F. Fraternali, E. Martinelli, Sustainable building material: recycled jute fiber composite mortar for thermal and structural retrofitting, in: O. Gervasi, B. Murgante, S. Misra, A.M.A.C. Rocha, C. Garau (Eds.), Computational Science and its Applications – ICCSA 2022 Workshops, Springer International Publishing, Cham, 2022, pp. 657–669, https://doi.org/10.1007/978-3-031-10545-6_44.

[27] I. Sanou, H. Bamogo, N. Sory, A. Gansoré, Y. Millogo, Effect of the coconut fibers and cement on the physico-mechanical and thermal properties of adobe blocks, Heliyon 10 (2024) e38752, https://doi.org/10.1016/j.heliyon.2024.e38752.

[28] N. Benmansour, B. Agoudjil, A. Gherabli, A. Kareche, A. Boudenne, Thermal and mechanical performance of natural mortar reinforced with date palm fibers for use as insulating materials in building, Energy Build. 81 (2014) 98–104, https://doi.org/10.1016/j.enbuild.2014.05.032.

[29] Y. Tong, W. Zhang, M. Li, T.T. Ngo, Q. Wang, W. Zeng, B. Li, Mechanical and thermal properties of structural lightweight bamboo fiber-reinforced insulating mortar, Case Stud. Constr. Mater. 22 (2025) e04462, https://doi.org/10.1016/j.cscm.2025.e04462.

[30] M.A. Albadrani, Strength development of PPC concrete with rice husk ash: optimal replacement levels for sustainable construction, Sustainability 17 (2025), https://doi.org/10.3390/su17188258.

[31] M. Stefanidou, P. Kampragkou, V. Kamperidou, Wood fibres as additives in mortars: a sustainable reinforcement, IOP Conf. Ser. Earth Environ. Sci. 1196 (2023) 012067, https://doi.org/10.1088/1755-1315/1196/1/012067.

[32] G. Ferrara, C. Caggegi, E. Martinelli, A. Gabor, Shear capacity of masonry walls externally strengthened using Flax-TRM composite systems: experimental tests and comparative assessment, Constr. Build. Mater. 261 (2020) 120490, https://doi.org/10.1016/j.conbuildmat.2020.120490.

[33] C. Menna, D. Asprone, M. Durante, A. Zinno, A. Balsamo, A. Prota, Structural behaviour of masonry panels strengthened with an innovative hemp fibre composite grid, Constr. Build. Mater. 100 (2015) 111–121, https://doi.org/10.1016/j.conbuildmat.2015.09.051.

[34] S. Khaleel, K. Madhavi, S.M. Basutkar, Mechanical characteristics of brick masonry using natural fiber composites, Mater. Today Proc. 46 (2021) 4817–4824, https://doi.org/10.1016/j.matpr.2020.10.319.

[35] A. Majumder, L. Canale, C.C. Mastino, A. Pacitto, A. Frattolillo, M. Dell'Isola, Thermal characterization of recycled materials for building insulation, Energies 14 (2021), https://doi.org/10.3390/en14123564.

[36] C.H. Koh, F. Gauvin, K. Schollbach, H.J.H. Brouwers, Investigation of material characteristics and hygrothermal performances of different bio-based insulation composites, Constr. Build. Mater. 346 (2022) 128440, https://doi.org/10.1016/j.conbuildmat.2022.128440.

[37] D. Hoxha, B. Ismail, A. Rotaru, D. Izabel, T. Renaux, Assessment of the usability of some bio-based insulation materials in double-skin steel envelopes, Sustainability 14 (2022), https://doi.org/10.3390/su141710797.

[38] C.C. Mastino, G. Concu, A. Frattolillo, Energetic performance of natural building materials: numerical simulation and experimental evaluation, Energies 17 (2024), https://doi.org/10.3390/en17040768.

[39] A. Atbir, M. Taibi, B. Aouan, A. Khabbazi, O. Ansari, M. Cherkaoui, T. Cherradi, Physicochemical and thermomechanical performances study for timahdite sheep wool fibers application in the building's insulation, Sci. Rep. 13 (2023) 5038, https://doi.org/10.1038/s41598-023-31516-9.

[40] L. Facconi, S.S. Lucchini, F. Minelli, B. Grassi, M. Pilotelli, G.A. Plizzari, Innovative method for seismic and energy retrofitting of masonry buildings, Sustainability 13 (2021), https://doi.org/10.3390/su13116350.

[41] T.C. Triantafillou, K. Karlos, K. Kefalou, E. Argyropoulou, An innovative structural and energy retrofitting system for URM walls using textile reinforced mortars combined with thermal insulation: mechanical and fire behavior, Constr. Build. Mater. 133 (2017) 1–13, https://doi.org/10.1016/j.conbuildmat.2016.12.032.

[42] T.C. Triantafillou, K. Karlos, P. Kapsalis, L. Georgiou, Innovative structural and energy retrofitting system for masonry walls using textile reinforced mortars combined with thermal insulation: in-plane mechanical behavior, J. Compos. Construct. 22 (2018) 04018029, https://doi.org/10.1061/(ASCE)CC.1943-5614.0000869.

[43] P.D. Gkournelos, T.C. Triantafillou, D.A. Bournas, Integrated structural and energy retrofitting of masonry walls: effect of In-Plane damage on the out-of-plane response, J. Compos. Construct. 24 (2020) 04020049, https://doi.org/10.1061/(ASCE)CC.1943-5614.0001066.

[44] K. Karlos, A. Tsantilis, T. Triantafillou, Integrated seismic and energy retrofitting system for masonry walls using textile-reinforced mortars combined with thermal insulation: experimental, analytical, and numerical study, J. Compos. Sci. 4 (2020), https://doi.org/10.3390/jcs4040189.

[45] E. Baek, D.A. Pohoryles, S. Kallioras, D.A. Bournas, H. Choi, T. Kim, Innovative seismic and energy retrofitting of wall envelopes using prefabricated textile-reinforced concrete panels with an embedded capillary tube system, Eng. Struct. 265 (2022) 114453, https://doi.org/10.1016/j.engstruct.2022.114453.

[46] P.D. Gkournelos, T.C. Triantafillou, Out-of-Plane behavior of In-Plane damaged masonry infills retrofitted with TRM and thermal insulation, J. Compos. Construct. 27 (2023) 04023054, https://doi.org/10.1061/JCCOF2.CCENG-4324.

[47] A. Khan, M. Khan, M. Ali, M. Khan, A.U. Khan, M. Shakeel, M. Fawad, T. Najeh, Y. Gamil, Predictive modeling for depth of wear of concrete modified with fly ash: a comparative analysis of genetic programming-based algorithms, Case Stud. Constr. Mater. 20 (2024) e02744, https://doi.org/10.1016/j.cscm.2023.e02744.

[48] M. Ali, L. Chen, Q.B.A.I.L. Qureshi, D.M. Alsekait, A. Khan, K. Arif, M. Luqman, D.S.A. Elminaam, A. Hamza, M. Khan, Genetic programming-based algorithms application in modeling the compressive strength of steel fiber-reinforced concrete exposed to elevated temperatures, Composites Part C: Open Access 15 (2024) 100529, https://doi.org/10.1016/j.jcomc.2024.100529.

[49] M. Ali, L. Chen, B. Feng, M.A. Rusho, M.B. Jelodar, F.D. Reyes Silva, J.L. Llamuca Llamuca, D.M. Tasán Cruz, N. Samandari, Thermal and dynamic response of hybrid fiber-reinforced concrete to fire exposure: experimental and computational approaches, Constr. Build. Mater. 478 (2025) 141397, https://doi.org/10.1016/j.conbuildmat.2025.141397.

[50] M. Ali, L. Chen, B. Feng, M.A. Rusho, M. Babaeian Jelodar, D.M. Tasán Cruz, W. Hussain, Coupled effects of thermal exposure and high strain rate on co_2 emissions of concrete structures: a comparative study of AI-driven emission signatures, Mater. Today Commun. 48 (2025) 113568, https://doi.org/10.1016/j.mtcomm.2025.113568.

[51] F. Stochino, A. Majumder, A. Frattolillo, M. Valdes, E. Martinelli, Jute fiber reinforcement for masonry walls: integrating structural strength and thermal insulation in sustainable upgrades, J. Build. Eng. 104 (2025) 112210, https://doi.org/10.1016/j.jobe.2025.112210.

[52] RILEM Technical Committee 232-TDT (Wolfgang Brameshuber), Recommendation of RILEM TC 232-TDT: test methods and design of textile reinforced concrete: uniaxial tensile test: test method to determine the load bearing behavior of tensile specimens made of textile reinforced concrete, Mater. Struct. 49 (2016) 4923–4927, https://doi.org/10.1617/s11527-016-0839-z.

[53] ACI 549.4R-13, Guide to Design and Construction of Externally Bonded Fabric-Reinforced Cementitious Matrix (FRCM) Systems for Repair and Strengthening Concrete and Masonry Structures, 2013.

[54] CNR-DT 215/2018, Guide for the Design and Construction of Externally Bonded Fibre Reinforced Inorganic Matrix Systems for Strengthening Existing Structures, 2019 (n.d.). Italy, https://www.cnr.it/en/node/12827. (Accessed 17 May 2026).

[55] ASTM E519/E519M-23, Standard Test Method for Diagonal Tension (Shear) in Masonry Assemblages, 2023.

[56] UNI EN ISO 9869-1:2014, Thermal insulation—Building elements—In-situ Measurement of Thermal Resistance and Thermal Transmittance, 2014.

[57] UNI EN ISO 8990:1996, Thermal insulation—Determination of steady-state Thermal Transmission properties—Calibrated and Guarded Hot Box, 1996.

[58] UNI EN ISO 10456:2008, Building Materials and products—Hygrothermal properties—Tabulated Design Values and Procedures for Determining Declared and Design Thermal Values, 2008.

[59] THE 17 GOALS | sustainable development, n.d, https://sdgs.un.org/goals. (Accessed 19 May 2026).

[60] G&P Intech S.r.l., FL-NET 300 BA: Rete Naturale in Fibra di Lino Apprettata, 2024. Technical Data Sheet NFL01, Rev. NFL01/02/24.

[61] L. Bacci, F. Camilli, S. Di Lonardo, P. Duce, E. Vagnoni, A. Mauro, Neglected wools: fundamental steps to counteract the loss of potentially valuable materials derived from native sheep breeds. Conference Papers in Materials Science 2013, 2013, pp. 1–7, https://doi.org/10.1155/2013/402372.

[62] Brebey – tecnologie con la lana, n.d, https://www.brebey.com/. (Accessed 24 August 2026).

[63] UNI EN 12667:2002, Thermal Performance of Building Materials and products—Determination of Thermal Resistance by Means of Guarded Hot Plate and Heat Flow Meter methods—Products of High and Medium Thermal Resistance, 2002.

[64] A. Majumder, F. Stochino, I. Farina, M. Valdes, F. Fraternali, E. Martinelli, Physical and mechanical characteristics of raw jute fibers, threads and diatons, Constr. Build. Mater. 326 (2022) 126903, https://doi.org/10.1016/j.conbuildmat.2022.126903.

[65] F. Stochino, A. Alibeigibeni, M. Zucca, M. Valdes, G. Concu, M. Simoncelli, M.A. Pisani, C. Bernuzzi, Mechanical behavior of composite slabs with recycled concrete aggregates: a preliminary study, Structures 70 (2024) 107838, https://doi.org/10.1016/j.istruc.2024.107838.

[66] A. Majumder, F. Stochino, A. Frattolillo, M. Valdes, G. Mancusi, E. Martinelli, Jute fiber-reinforced mortars: mechanical response and thermal performance, J. Build. Eng. 66 (2023) 105888, https://doi.org/10.1016/j.jobe.2023.105888.

[67] EN 13501-1:2018, Fire Classification of Products and Building Elements - Part1: Classification Using Data from Reaction to Fire Tests, 2019.

[68] EN 1015-2, Methods of Test for Mortar for Masonry—Part 2: Bulk Sampling of Mortars and Preparation of Test Mortars, 2007.

[69] EN 1015-3, Methods of Test for Mortar for Masonry—Part 3: Determination of Consistence of Fresh Mortar (By Flow Table), 2007.

[70] EN 1015-11:2019, Methods of Test for Mortar for masonry—Part 11: Determination of Flexural and Compressive Strength of Hardened Mortar, 2019.

[71] A. Alibeigibeni, F. Stochino, M. Zucca, F.L. Gayarre, Enhancing concrete sustainability: a critical review of the performance of recycled concrete aggregates (RCAs) in structural concrete, Buildings 15 (2025) 1361, https://doi.org/10.3390/buildings15081361.

[72] UNI EN 1934, 2000, Thermal Performance of buildings—Determination of Thermal Resistance by Hot Box Method Using Heat Flow meter—Masonry, 2020.

[73] UNI EN ISO 6946:2018, Building Components and Building elements—Thermal Resistance and Thermal transmittance—Calculation Methods, 2018.

[74] G. Marcari, M. Basili, F. Vestroni, Experimental investigation of tuff masonry panels reinforced with surface bonded basalt textile-reinforced mortar, Compos. B Eng. 108 (2017) 131–142, https://doi.org/10.1016/j.compositesb.2016.09.094.

[75] D. Ungureanu, N. Țăranu, D.A. Ghiga, D.N. Isopescu, P. Mihai, R. Cozmanciuc, Diagonal tensile test on masonry panels strengthened with textile-reinforced mortar, Materials 14 (2021) 7021, https://doi.org/10.3390/ma14227021.

[76] M. Shabdin, M. Zargaran, N.K.A. Attari, Experimental diagonal tension (shear) test of Un-Reinforced Masonry (URM) walls strengthened with textile reinforced mortar (TRM), Constr. Build. Mater. 164 (2018) 704–715, https://doi.org/10.1016/j.conbuildmat.2017.12.234.

[77] P.D. Gkournelos, T.C. Triantafillou, D.A. Bournas, Integrated structural and energy retrofitting of masonry walls: effect of In-Plane damage on the out-of-plane response, J. Compos. Construct. 24 (2020) 04020049, https://doi.org/10.1061/(ASCE)CC.1943-5614.0001066.

[78] F. Stochino, A. Majumder, A. Frattolillo, M. Valdes, M. Sassu, F. Mistretta, Structural and thermal performance of masonry walls: insights from TRM-based upgrading techniques, Structures 81 (2025) 110200, https://doi.org/10.1016/j.istruc.2025.110200.

[79] A. Furtado, H. Rodrigues, A. Arêde, H. Varum, A experimental characterization of seismic plus thermal energy retrofitting techniques for masonry infill walls, J. Build. Eng. 75 (2023) 106854, https://doi.org/10.1016/j.jobe.2023.106854.

[80] L. Facconi, S.S. Lucchini, F. Minelli, B. Grassi, M. Pilotelli, G.A. Plizzari, Innovative method for seismic and energy retrofitting of masonry buildings, Sustainability 13 (2021), https://doi.org/10.3390/su13116350.

[81] F. Longo, A. Cascardi, P. Lassandro, M.A. Aiello, Energy and seismic drawbacks of masonry: a unified retrofitting solution, J Build Rehabil 6 (2021) 31, https://doi.org/10.1007/s41024-021-00121-6.

[82] P.D. Gkournelos, T.C. Triantafillou, Out-of-Plane behavior of In-Plane damaged masonry infills retrofitted with TRM and thermal insulation, J. Compos. Construct. 27 (2023) 04023054, https://doi.org/10.1061/JCCOF2.CCENG-4324.